nature portfolio

Peer Review File

Delineating the Stepwise Millisecond Allosteric Activation Mechanism of the Class C GPCR Dimer mGlu5

REVIEWER COMMENTS

Reviewer #1 (Remarks to the Author):

In the present study, the authors utilized mGluR5 as a prototypical example for investigating dimeric GPCRs activation. They employed a computational framework incorporating the transition pathway generation algorithm NEB to sample 13 structures along the MEP, followed by 10 1μs unbiased MD runs for each structure (130 μs in total) to disclose mGluR5 dynamic activation landscape. After the MSM analysis of the comprehensive simulations, they identified a stepwise allosteric activation of mGluR5 in ~3.5 ms, which is consistent with the recently reported stepwise conformational arrangement of mGluR2 by Reza Vafabakhsh et al (Nat Chem Biol. 2021;17(3):291-297). Furthermore, the study revealed a dynamic portrait of the three functional domains of mGluR5 at an atomic scale, capturing an intermediate Rco state of the VFT domain, a crucial apical module of the CRD, and the dynamic allostery within the 7TM domains. They further validated the apical module of the CRD and several micro-switches in the 7TM through alanine mutagenesis, thus provided more conformation changes details of these critical regions.

In essence, the provided analysis is indeed interesting, offering new insights into the dynamic activation mechanism of a dimeric GPCR, and the proposed computational workflow is really appealing. I have the following minor concerns:

1.The mGluR5 structure in PDB 6N51 is stabilized by a nanobody. Whether the nanobody is removed for the extended MD?

2.Figure 2A: What criteria do you employ to distinguish between Protomer A and Protomer B, considering their equivalence in a homodimer?

3.Page 7, Line 188: In defining the compaction movement of the VFTs, you use the COM of the LB2 of each VFT. Why not consider the electrostatic interactions between charged residues in the lower lobe as explored in Nature, 2015, 524(7566):497-501.

4.Figure 4: The two possible conformational orientations mentioned in the text better be labeled in the Figure 4A.

5.Page 12, Lines 346-347: How do you design the nine clustered mutations at the B2' module? What not just using single point mutations? I think nine clustered mutations maybe too much.

6.Figure 5: All superscripts and subscripts in the legend are incorrectly formatted—for example, dTM6-TM6, E7706.35A, etc. Additionally, in Figure 4D, M7786.43 should be accurately annotated as M7786.43B.

7.Figure 6: Highlighting the regions of correlated motions would improve readability.

8.Prof.Brian K Kobilka also just provided a step-wise activation model of mGluR5 by Cryo-EM(Step-wise activation of a Family C GPCR, BioRxiv), I think you should cite and discuss the paper.

Reviewer #2 (Remarks to the Author):

Delineating the Stepwise Millisecond Allosteric Activation Mechanism of the Class C GPCR Dimer mGluR5

Mingyu Li, Xiaobing Lan, Xinchao Shi, Chunhao Zhu , Xun Lu, Jun Pu, Jian Zhang, Shaoyong Lu

This article uses extensive computational molecular dynamic simulations to elucidate the full pathway for activation of the mGlu5 receptor dimer. Large scale simulations are used and analysed to identify the meta-stable states, and the kinetic transitions and pathway that connect the key states. Thus, the pathway is proposed to occur on an overall timescale of approx. 3ms, a result that corresponds well with the expected activation time based on experiment. The analysis is extensive and points out the key interactions and motifs that characterize each state and transition.

Since the recent breakthroughs in experimental structures of mGlu receptors there has been a growth in possible computational studies. This is a good example of using the available structures and a thorough computational approach to probe a question which is beyond the scope of experiment, namely the full characterization of the activation pathway and it's intricate details and intermediates. The work is of value to the field and the wider GPCR research community, it also serves as a fine example of MD and computational simulations used to a high standard to reveal new insights.

The work is well planned and structured. The methods chosen are appropriate, full atom MD methods are needed for the appropriate accuracy and detail to correctly predict the pathway, as this reviewer notes that other smaller scale studies have revealed important cascade effects arising from specific side chain motions and interactions. The large number of computational effort of the simulations is a requirement, and one should note that the size of the computational system here is very large compared to other simple enzyme systems, in other words, it would have been a major undertaking to run 130 us of simulation. The tICA and MSM work is well performed and appropriate. It represents the state of the art for revealing pathways and kinetic states as required here. The analysis and illustration of the results (figures etc) is well presented. The text is very well written.

The reviewer considers the work to have been performed to a high standard, and there are no apparent doubts or questions regarding data quality etc. The authors have been responsible for similar studies in recent (approx. 5 years) suggesting the work is backed up by extensive experience in the field of computational simulation and interface with biological mechanisms and understanding.

Recommendations:

The work is complete and publishable in its current form. Here are some suggestions and recommendations:

A key therapeutic approach to modulating mGlu receptor function has small molecule allosteric modulation, indeed mGlu5 receptor NAMs and PAMs have reached clinical trials. Would simulations performed with allosteric modulators in place reveal more insights relevant for drug discovery? If the authors don't consider it necessary to perform simulations with synthetic ligands, it would certainly be of interest to discuss in more detail how the findings of other simulation-based studies, that have used different allosteric modulations. The current work discusses nicely the conformational/activation switches but doesn't venture into commenting on the meaning or validity of how the allosteric modulators interact with those switches, do those hypotheses remain valid?

There are some interesting cases in the literature of amino acids that were mutated and shown to be important for mGlu receptor activity, and allosteric activation, however, they were neither located in the orthosteric or allosteric binding sites. They were in positions 4.51a.41c and 4.52a.42c (and there may be other examples). Are the authors able to rationalize the relevance of these amino acids in their work?

Make all data and structures available. The input structures and the key intermediate states.

The accepted IUPHAR/BPS nomenclature for mGlu receptors is to write as mGlu5 receptor, where the 5 is a subscript, not mGluR5 which is a legacy abbreviation. Recommend changing to the new accepted version.
https://www.guidetopharmacology.org/GRAC/ObjectDisplayForward?objectId=293

Reviewer #3 (Remarks to the Author):

The manuscript by Li et al. investigates the challenging problem of mGluR5 dimer activation and reports a Markov State Model (MSM) of based on 130 μs of all-atom MD simulations. A Nudged Elastic Band (NEB) analysis was first performed to generate 13 conformational states that connect the inactive and active states (cryoEM structures). Then, 10 μs of MD simulations were carried out on each state to finally construct the MSM model. I appreciate the approach chosen, which has the potential to yield a comprehensive understanding of this complex system. However, the data at hand are inadequate for assessing the quality of the proposed MSM model, which seems insufficient in describing the intricacies of activation dynamics. There are 3 major concerns:

1. NEB model.

Limited data are provided to ensure the reliability of the simulated transition pathways. While it is difficult to estimate the number of intermediates needed here, one may expect that larger numbers are necessary to describe the conformational changes of such a flexible multi-domain dimer. This naturally comes with higher computational costs for the subsequent MSM model construction. I suggest running NEB calculations with varying numbers of images to assess the convergence and pathway quality.

2. MSM model.

The choice of the MSM hyperparameters (e.g. 2 tICs, 300 microstates and 1 ns lag time) is unjustified. This makes it difficult to evaluate the model's qualilty. Given the complexity and slow dynamics of the system, 2 tICs and 1 ns lag time are probably insufficient. The author may use variational approach for Markov processes (VAMP2) or Generalized matrix Rayleigh quotient (GMRQ) scores in a cross validation to determine the numbers of tICs and microstates required. An example can be found in Westerlund et al. Plos Comput Biol 2022.

The tICA was performed on "the coordinates of Cα of mGluR5". More details are necessary about how the tICA was performed and why 2 tICs were used for the MSM.

Therefore, although the ITS validation in Fig S1 appears satisfying (which timestep is used?), 2 tICs and 1 ns lag time are likely too short for a system with both fast and slow dynamics.

3. Experimental validation

I acknowledge that the authors performed site-directed mutagenesis to examine 4 microswitches in sensitive regions. Although microswitches are an important aspect of GPCR activation, the primary issue with the manuscript is the credibility of the overall model of mGluR5 activation.

A preprint posted by the Kobilka lab in August (https://doi.org/10.1101/2023.08.29.555158) has captured several intermediate states by cryoEM/smFRET that illustrate the stepwise activation. A more recent preprint describes similar intermediate states even for PAM-bound structures (https://doi.org/10.1101/2023.11.07.565819). The intermediate-state structures are available for comparison with the models proposed in this manuscript. In particular, activation of the ECD appears uncoupled (or loosely coupled) to that of the 7TM. This does not seem to be the case here.

Concerning the activation kinetics, the MSM model here suggests a timescale of ~2 ms which "is in agreement with the experimentally validated activation timescale of 1–2 ms for the mGluR1 homodimer" (p. 7, l. 177-179). Several questions arise from this statement:

- the 2 ms timescale in the mGluR1 study (M. Lohse lab 2019) referred to the intramolecular motions of the 2 protomers, whereas the activation of the 7TM was much slower (~ 20 ms). The latter is presumably associated with G protein coupling, beyond the scope of this manuscript. However, the 2 processes should be specified to avoid confusion. The prepint from the Kobilka lab has shown that 7TM undergoes further conformational changes in the presence of G proteins (unlike mGluR2). Therefore, mGluR5 activation within 7TM also involves 2 processes, the intramolecular motions (protomer approximation) and intramolecular TM conformational changes triggered by G protein binding.

- in the case of mGluR2 (Olofsson et al. Nat Commun 2014), merely the ECD dimer activation takes > 4 ms. The full-length dimer activation may be even slower.

Different mGluR subtypes show different apo states and conformational changes upon activation. It is highly speculative to assume the same activation timescales for different mGluRs.

While this work holds promise, a substantial volume of aditional simulations and analyses are necessary to achieve a convincing MSM model. Only then can one evaluate the results and discussions on the detailed motions and microswitches. I regret that the manuscript in its current form does not meet the standards required for publication in Nat Commun.

Reviewer #4 (Remarks to the Author):

The purpose of the study from Li et al is to provide insights into the activation mechanism of mGlu5 receptor, a homodimer complex belonging to class C family of G-protein coupled receptors. More precisely, the authors wish to describe the transition states and timescale along the conformational landscape of the activation process. It may be that the modeling approach allows to capture transition states that are not stable enough to be captured by structural or biophysical methods.

The manuscript relies on predictive modeling of intermediate states between the resting and active conformations of mGlu5 receptor homodimer. For the starting and final conformations, the authors used the coordinates of two cryo EM structures described in Koehl et al Nature 2019 (PDB ID 6N52 and 6N51). A major challenge is to comprehend a process that occurs on a millisecond scale when molecular modeling is usually limited to microsecond events.

The authors first defined the minimum energy path (MEP) between the resting and active states of full-length mGlu5 receptor. Then molecular dynamics (MD) simulations in explicit solvent models were ran for 13 conformations identified at the previous step and distributed along the activation pathway. Next, time-structure-based independent component analysis (tICA) was applied to the MD trajectories and allowed the identification of five metastable states S1 to S5. Representative conformations of these 5 states along the transition pathway from Resting to Active agonist bound, are then thoroughly analyzed in a large part of the manuscript.

Comments

1) Five sequential metastable states S1 to S5 were identified along the activation pathway of mGlu5 receptor. Representative structures of these five states were then characterized.

S1 and S5, represent the initial and last conformations of the activation process, corresponding to the inactive and active agonist bound cryo-EM structures (PDB ID 6N52 and 6N51). Thus, the interest is in the S2, S3 and S4 intermediate conformations and the kinetics of the whole activation pathway.

The authors first describe the changes of the whole dimer and kinetics aspects. They observe an asymmetrical dimer arrangement in 200µs between S1 and S2, a rate-limiting step of 2.14 ms to reach S4 and a total of 3.54 ms from S1 to S5 when activation is initiated by glutamate binding. They claim that a similar time scale has been experimentally observed by Olofsson et al (ref 39) for the VFT domain and by Grushevskyi et al (ref 35) for the whole pathway. Although the sub-milliseconds of the VFT activation is indeed well known since the work of Olofsson et al in 2014, it is more questionable for the whole pathway to the active agonist bound state. For mGlu1 receptor, Grushevskyi et al identified two metastable intermediate states that are reached in sub-

milliseconds for the first one and 1ms for the second but it takes about 20 ms to switch to the fully active conformation. Rondard and Pin (Cur Op Pharmacol 2015) when summarizing several studies, mention 35 ms to get to the second metastable state (a conformation with a first relative rearrangement of the two 7TMs) and 50 ms for the full activation. Recent studies show that interaction with the G-protein (which happens in cells) in the fully active state extends the timescale for full activation. Yet the authors of the present manuscript should give more support to the rather short time between S1 and S5 that they calculated.

2) Then the authors detailed the fold of protomer A and B in the different states.

For the first state S1, they find both protomers holding an open VFT and a dimer conformation close to the 6N52 structure. Quisqualate had been replaced by glutamate which binds to the upper lobe of the VFT. Surprisingly, the α-carboxylate of glutamate is not binding to the conserved Ser152 and Thr175 of the upper lobe as in the X-Ray structure 1EWK:B. These two residues are bound to the α-carboxylate of agonists/antagonists in all VFT structures, open or closed. See for example mGlu1 VFT bound to LY341495 or to MCPG in 3KS9 and 1ISS respectively. In these structures the γ-carboxylate interacts with a conserved Lys and Tyr in group I of mGluRs (K409/K396 and Y74/Y64 in mGlu1 and mGlu5 respectively). Lys409/Lys396 is a conserved Lys all through the 8 mGlu receptors and always making a salt bridge with the γ-carboxylate of agonists/antagonists deriving from glutamate. Thus in the first S1 conformation, the docking of glutamate is inverted (Figure S3). This wrong initial docking must have major consequences in the other conformations. Indeed in the following state S2 (Figure S4) the α-carboxylate of glutamate makes salt bridges with Lys396, Arg68 (protomer A) and Arg310 (protomer B) which are well known to interact with the γ-carboxylate. This inversion of glutamate and derivatives is quite common when carrying out dockings and one should be careful in choosing the poses. In the S3 state, the classical docking is recovered with the α-carboxylate of glutamate making H-bonds with Ser152 and Thr173. Thus S1 an S2 conformations bound to glutamate are questionable. In particular it is strange that glutamate bound to the closed protomer B of state 2 twists around in S3. The authors should check their dockings and if they confirm the S1 and S2 dockings explain why they do not comply with all published structures and 3D-models.

3) A paragraph is focused on the analysis of the CRD domains that link the VFT and 7TM domains in each protomer. The authors found that the CRD module bound to the VFT displays more flexibility than the module linked to the 7TM as previously observed (see for example Liauw et al Nature Com 2021 demonstrating “VFT and CRD domains loosely coupled”). It is not clear which of the intra-domain CRD conformations observed during the simulations (Figure 4) are found in which of the S1 to S5 states. Regarding the inter-domain conformational arrangement of the CRDs, the elaborated study from Liauw et al (Nature Com 2021) defined four states that are claimed to coincide with S1 to S4 of the present study. However there seems to be a discrepancy in particular the S1 state in Figure S7 does not seem to correspond to the initial symmetrical resting conformation. This needs to be clarified.

To support their results, the authors introduced some mutations from Arg524 to Trp532 and performed functional assays but they did not enumerate in what residues they were mutated into. This needs to be added and interpreted according to the mutations.

4) When introducing the analysis of the 7TM domain dynamics of their work, the authors recall the TM6–TM6 interface reorientation and the G-protein binding cavity. The cited references are incomplete. They should cite and comment on the recent cryo-EM mGlu5 structures disclosed in a recent article from the Kobilka's group (Kumar et al BioRxiv 2023 and structures available at the Protein Data Bank). They should also better report on the stabilizing role of G-protein and positive allosteric modulators (e.g. Cao et al Nature Com 2021, Lecat-Guillet et al Sci Adv 2023, Cannone et al BioRxiv2023) besides a comment on "dynamic allostery" and citing reference 43.

When monitoring the conformational orientations of the TM6–TM6 interface, the authors identified three metastable states (M1, M2, and M3). They need to link these states to the S1 to S5 states defined previously in the manuscript. Is M4 in Figure 5C corresponding to M3, it is not mentioned in the text? A transit intermediate between M1 and M2 is also cited. Altogether, data in this paragraph are not well presented. It needs to be improved.

It is now admitted that a fully active state of mGluRs can only be reached when a G-protein is bound to the receptor. Can the G-protein be added in the models? This would give a better insight into the activation mechanism from resting to fully active state. Moreover, the functional assays with the various mutants are run in HEK293T cells where the G-protein is present.

The reported results should be compared to the recent cryo-EM structures and the sequential mGlu5 activation pathway recently disclosed. The authors should put forward what new information they provide with a molecular modeling approach in comparison to the structural and biophysical approaches.

5) The correlation map to analyze movements between domains in the course of a biological pathway is a very powerful tool. Indeed Figure 6 provides a long range connection between the VFT and the 7TM domains and between the adjacent protomers in the dynamics. Yet, since the binding of glutamate may not be correct in S1 and S2, the analysis may not be relevant.

Figure 6B does not give additional information compared to panel A.

6) In the discussion, putting forward that class C GPCRs dimerization may be useful for all GPCRs is not true because the mechanisms are quite different.

According to recent literature, active and fully active conformations of mGlu receptors should be distinguished.

In the first part of the manuscript, 5 states S1 to S5 are found and analyzed. Then in the discussion, the results are summarized in Figure 7 with only 4 states. This should be explained.

This cartoon is very similar to that of Liauw et al Nature Chem Biol 2021 (Figure 5). This similarity should be commented.

Specific comments

1) In Cao et al (Nature Com 2021) and Kumar et al (BioRxiv2023), the crucial type of membrane lipids used in assays is exposed. The authors used the classical POPC to simulate the bilayer membrane. They should check the impact of this choice on the kinetics.

2) In all figures where a free energy profile is displayed, the color scale should be mentioned in the legend. Same remark for the scale in Figure S9

Simulations should be able to describe the film and kinetics of the pathway between 3D-structures provided by structural biology. But the multiple virtual steps need to be validated. In the work of Li et al, an interesting approach is used but some results are questionable.

Altogether this manuscript lacks of clarity and rigor. The authors need to show better what critical information they provide in comparison to that from literature.

REVIEWER COMMENTS

Reviewer #1 (Remarks to the Author):

In the present study, the authors utilized mGlu5 as a prototypical example for investigating dimeric GPCRs activation. They employed a computational framework incorporating the transition pathway generation algorithm NEB to sample 13 structures along the MEP, followed by 10 1μs unbiased MD runs for each structure (130 μs in total) to disclose mGlu5 dynamic activation landscape. After the MSM analysis of the comprehensive simulations, they identified a stepwise allosteric activation of mGlu5 in ~3.5 ms, which is consistent with the recently reported stepwise conformational arrangement of mGluR2 by Reza Vafabakhsh et al (Nat Chem Biol. 2021;17(3):291-297). Furthermore, the study revealed a dynamic portrait of the three functional domains of mGlu5 at an atomic scale, capturing an intermediate Rco state of the VFT domain, a crucial apical module of the CRD, and the dynamic allostery within the 7TM domains. They further validated the apical module of the CRD and several micro-switches in the 7TM through alanine mutagenesis, thus providing more conformation changes details of these critical regions.

In essence, the provided analysis is indeed interesting, offering new insights into the dynamic activation mechanism of a dimeric GPCR, and the proposed computational workflow is really appealing.
RESPONSE: Thank you for your affirmation of our work, and your insightful suggestions from an experimental view obviously improved the quality and credibility of our manuscript. Following your suggestions, we have carefully revised the manuscript and performed additional experiments to validate in silico findings. We hope our detailed responses address your comments.

I have the following minor concerns:

1.The mGlu5 structure in PDB 6N51 is stabilized by a nanobody. Whether the nanobody is removed for the extended MD?
RESPONSE: Yes, the nanobody was removed in the MD simulations, which has described in the revised method section.

2.Figure 2A: What criteria do you employ to distinguish between Protomer A and Protomer B, considering their equivalence in a homodimer?
RESPONSE: To more accurately describe the asymmetric dynamics of the two protomers during our simulations, we distinguish between the protomer A and B using the molecular chain ID recorded in both the inactive (PDB ID: 6N52) and active (PDB ID: 6N51) cryo-EM structures. In inactive and active cryo-EM structures, the two protomers are typically indistinguishable, exhibiting nearly identical conformations at the per-residue level. This asymmetry hinders the elucidation of the underlying dynamic activation pathway. Notably, we unveiled the dynamic asymmetric activation pathway

using massive MD simulations. For example, since one glutamate first established interactions with the VFT domain from the protomer B during our simulations, it closed first than the other VFT from the protomer A, resulting in a transient intermediate Rco conformation (Figure 3).

3.Page 7, Line 188: In defining the compaction movement of the VFTs, you use the COM of the LB2 of each VFT. Why not consider the electrostatic interactions between charged residues in the lower lobe as explored in Nature, 2015, 524(7566):497-501.

RESPONSE: Thank you for your valuable insights. As your comment, Vafabakhsh et al. (*Nature*, **2015**, 524(7566):497-501) identified a conserved positively charged lysine (K240 in mGlu2) in stabilizing the active interface between the LB2s. Replacing the COM distance of the LB2s with the distance between the analogous lysine residues (K247 in mGlu5) yielded a remarkably similar free energy surface (Figure R1). However, in our option, to describe the compaction movement of the VFT domains, it is more robust to use a domain-level descriptor (distance between the COMs of the LB2 of each VFT) rather than a residue-level descriptor (distance between K247 residues). Nevertheless, the similarity in the new free energy surface further substantiates the robustness of our choice of the descriptor and the validity of the identified dynamic activation pathway.

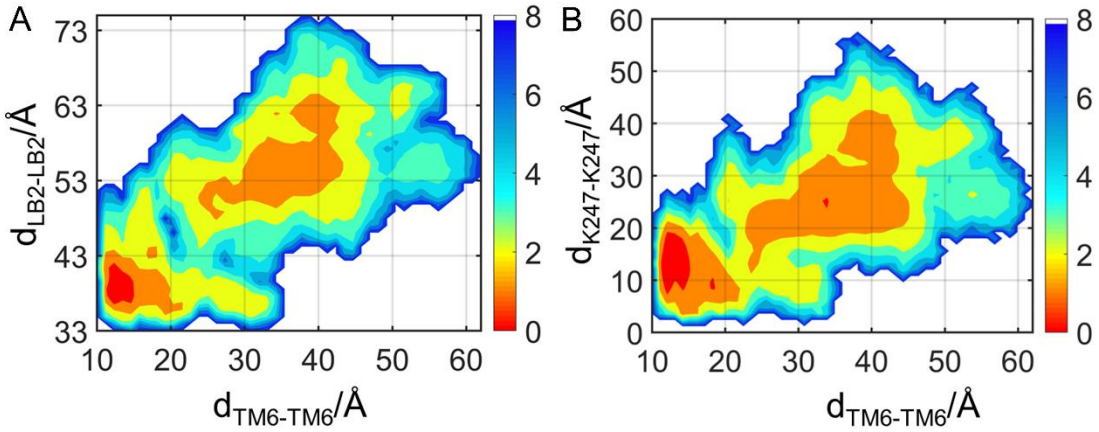

Figure R1. Free energy surfaces to reflect the compaction movement between the VFT and 7TM domains. The VFT movement is measured by the distance between the COMs of the LB2(A) or the crucial inter-protomer electrostatic interaction between K247 (B).

4.Figure 4: The two possible conformational orientations mentioned in the text better be labeled in the Figure 4A.

RESPONSE: That is a good suggestion, and we have accordingly labeled the two possible conformational orientations with arrows to enhance clarity.

5.Page 12, Lines 346-347: How do you design the nine clustered mutations at the B2' module? What not just using single point mutations? I think nine clustered mutations maybe too much.

RESPONSE: Thank you for this critical comment. To address this concern, we further designed a cysteine-mediated crosslink (I523C) to confirm the role of the B2' module

in mediating the active CRDs interface. As shown by the replotted Figure 4C and D, the I523C mutant maintained comparable levels of cell surface expression but demonstrated a robust constitutive activity as high as the glutamate-induced activity in the wild type (WT). Mutating the I523 residue to alanine (I523A) or altering its adjacent two residues (K521&V522&I523A, I523&R524&K525A) led to the absence of constitutive activity and a significant reduction in efficacy, yet cell surface expression levels remained similar to those of the WT. These experiments clearly confirmed the active CRDs interface mediated by B2' modules without introducing too many mutations. We have added these results in the revised main text.

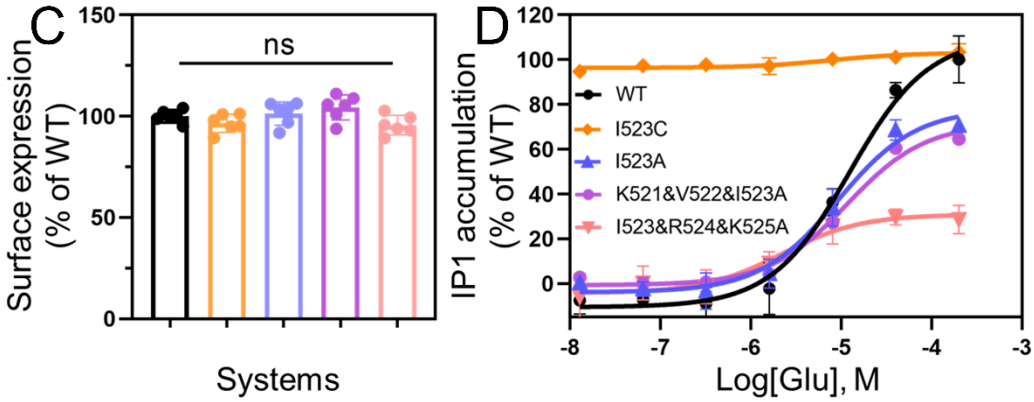

Figure 4. Experimental verification of the observed CRD association dynamics. (C) Quantification of cell surface expression. Data are presented as mean ± s.e.m. of six independent experiments. ns, not statistically significant (one-way ANOVA with Dunnett's post hoc test). (D) Crosslinking at the potential surface of the B2' module by an I523C mutant displays high constitutive activity, as measured using IP accumulation. Alanine mutation of critical residues involved in forming the observed B2'-mediated interface blunt glutamate-induced signaling compared to the WT. Data are presented as mean ± s.e.m. of three independent experiments.

6.Figure 5: All superscripts and subscripts in the legend are incorrectly formatted—for example, dTM6-TM6, E7706.35A, etc. Additionally, in Figure 4D, M7786.43 should be accurately annotated as M7786.43B.

RESPONSE: Thanks for bringing these typing errors to our attention. These typos have been corrected, and we have carefully revised the manuscript again to avoid typos.

7.Figure 6: Highlighting the regions of correlated motions would improve readability.

RESPONSE: We replotted Figure 6, and the regions of correlated motions are highlighted by black squares.

8.Prof.Brian K Kobilka also just provided a step-wise activation model of mGlu5 by Cryo-EM(Step-wise activation of a Family C GPCR, BioRxiv); I think you should cite and discuss the paper.

RESPONSE: We agree with your suggestions. Kumar et al. have released four cryo-EM structures of mGlu5, including Quis-bound intermediate 1a (PDB ID: 8T7H), Quis-

bound intermediate 2a (PDB ID: 8T8M), Quis and CDPPB-bound intermediate 3a (PDB ID: 8TAO), and CDPPB-bound inactive intermediate 1b (PDB ID: 8T6J). Although Cannone et al. have not released their structures, we can still compare through their article. Next, let us compare the recently determined intermediate-state structures with our proposed models one by one.

(1) **Quis-bound Intermediate 1a:** The Intermediate 1a exhibits an Rcc conformation, characterized by two closed VFTs domains while the CRDs and 7TMs remain as far apart as in the inactive mGlu5 state. In alignment with this, our in-depth analysis of the S2 metastable state identified an alternative configuration of the VFTs (denoted as S2', minimal Cα RMSD to Intermediate 1a: 3.8 Å), in which the VFT of protomer A transitioned from an open (S2, Rco) to a nearly closed state ($RMSD_{VFT}^{A}$ = 1.8 Å), closely approaching an Rcc conformation (Figure 3B). Moreover, Cannone et al. have captured a transient and non-classic binding pose of quisqualate (a glutamate analogue) in the Rcc conformation of mGlu5. Similarly, our simulations also captured the dynamic binding poses of glutamate, particularly within the S2 state (Figure S4), highlighting the substantial flexibility of the VFT domains. We have added the comparison in the revised manuscript accordingly throughout the text and figures (Figure 3 and Supplementary Note 4)

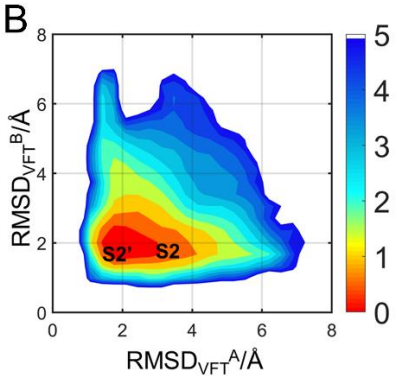

Figure 3B. A per-protomer analysis of the S2 metastable state uncovered an alternative configuration of the VFTs, termed S2'.

(2) **Quis-bound Intermediate 2a:** The Intermediate 2a, simultaneously stabilized by Quis and Nb43 exhibits a conformation remarkably similar (Cα RMSD = 2.3 Å) to the structure of 6N51 (also complexed with Quis and Nb43) determined by the Kobilka lab in 2019. Both structures are similar to the S5 through our simulations (minimal Cα RMSD = 2.2 Å).

Significantly, our simulations uncovered two additional metastable states, S3 and S4, which might bridge the Intermediate 1a and 2a. These transient metastable states may prove challenging to stabilize by cryo-EM. In these metastable states, we revealed the role of the B2' module in mediating the active CRDs interface. This active CRDs interface was confirmed by introducing a cysteine-mediated crosslink at the potential interface of the B2' module (I523C) (See the response above).

(3) **Quis and CDPPB-bound Intermediate 3a:** Kumar et al. observed an asymmetric TM6-TM6 interface in Intermediate 3a, highlighting the critical asymmetric microswitch $Y799^{6.44}$. These asymmetric features, although absent in earlier apo

(PDB ID: 6N52) and active (PDB ID: 6N51) mGlu5 structures that are endpoints of our simulations, have been successfully captured in our extensive simulations. The critical role of $Y799^{6.44}$ in receptor activation has been confirmed through our site-directed mutagenesis experiments (Figure 5).

In addition, Kumar et al. failed to determine the ICL2 conformation in the cryo-EM structure of Intermediate 3a. Utilizing Bimane fluorescence, they observed a notable conformational change in the ICL2 upon the addition of CDPPB, distinguishing this effect from that observed with the agonist alone. Although the sensor revealed discrete conformations of ICL2 upon PAM binding, it did not resolve ICL2 structural compositions. To delve deeper into how the PAM impacts the dynamics of the mGlu5 activation and further extend our model of mGlu5 activation, leveraging the cryo-EM structure (Intermediate 3a), we conducted unbiased all-atom MD simulations (1 μs × 10 independent MD simulations) on full-length mGlu5 system bound with agonist glutamate and PAM CDPPB. Combined with the prior extensive simulation trajectories (1μs × 10 × 13 NEB replicas), we generated the FEL of ICL2 (Figure S14 C and D). It unveiled that ICL2 existed in a dynamic equilibrium, fluctuating between "closed" or "collapse" states that may occlude the intracellular cavity, and "open" or "extended" states that could facilitate receptor-effector interactions and promote receptor activation. The presence of glutamates alone failed to significantly affect this equilibrium, suggesting that orthosteric agonists by themselves were insufficient to stabilize an active ICL2 conformation. In contrast, the addition of CDPPB to the glutamate-bound mGlu5 markedly shifted the equilibrium toward an active ICL2 state, characterized by an appropriately open and extended conformation. Consequently, we proposed that PAM binding transitioned ICL2 from inactive closed or collapsed states, which might impede G_q protein binding, to active open and extended states. The detailed information has been updated as a supplementary information part (Supplementary Note 6).

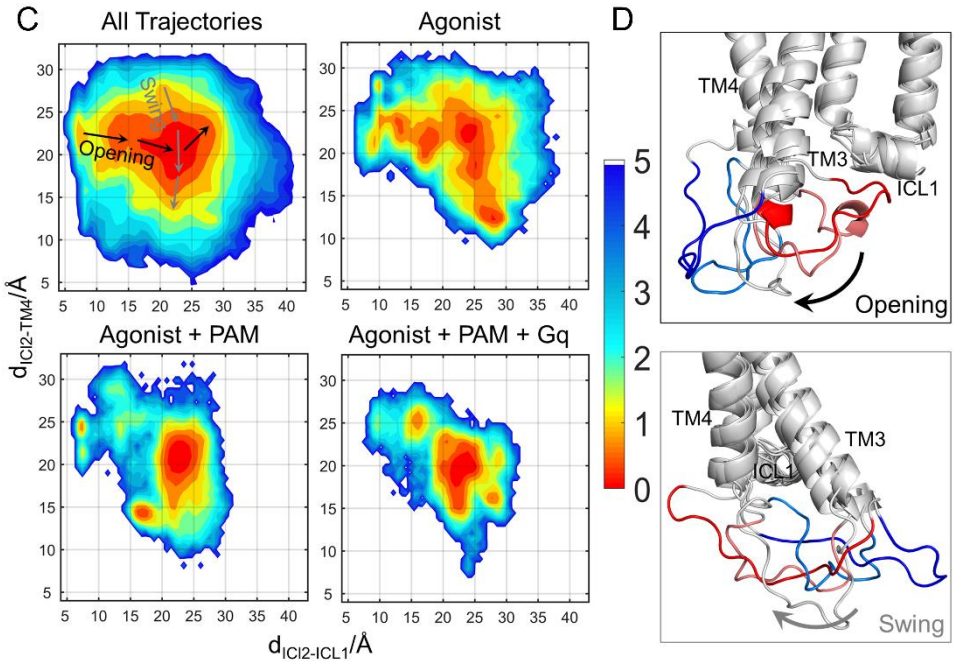

Figure S14. Conformational changes upon CDPPB binding to the mGlu5. (C) The conformational landscape of ICL2 derived from simulations. The *x*-axis ($d_{ICL2\text{-}ICL1}$) was defined as the distance between the Ca atom of C681 on the ICL2 and the center of mass (COM) of all Ca atoms of ICL1, reflecting the opening motion of ICL2 with increasing $d_{ICL2\text{-}ICL1}$ values. The *y*-axis ($d_{ICL2\text{-}TM4}$) was determined using the distance between the Ca atoms of C661 on the ICL2 and $C691^{4.30}$ on the TM4, the same points of the fluorescence experiments, representing the swinging motion of ICL2. (D) Representative structures of mGlu5, showcasing the varied conformations of ICL2.

(4) **CDPPB-bound inactive Intermediate 1b:** Although Intermediate 1b is beyond the scope of our research, it inadvertently validated the moderate inter-domain dynamics within the CRDs, even when mGlu5 is inactive, as demonstrated in our simulations (Figure S8). The profiling of CRDs inter-domain dynamics—quantified by the distance between residues D560 across both protomers—revealed that, even in the inactive state, 97% of the conformations can fluctuate from 68.0 Å to 78.0 Å. In the apo inactive cryo-EM structure, the distance is 68.3 Å (PDB ID: 6N52). In the antagonist-bound inactive cryo-EM structure, the distance is 70.2 Å (PDB ID: 7FD9) (Nasrallah et al., *Cell Rep*, **2021**, 36(9):109648). In the Intermediate 1b (PDB ID: 8T6J), the distance is 73.4 Å, which is close to the metastable state S1 (74.3 Å). This variability highlights the inherent flexibility within the CRDs, even in states traditionally considered inactive.

Reviewer #2 (Remarks to the Author):

This article uses extensive computational molecular dynamic simulations to elucidate the full pathway for activation of the mGlu5 receptor dimer. Large scale simulations are used and analysed to identify the meta-stable states, and the kinetic transitions and pathways that connect the key states. Thus, the pathway is proposed to occur on an overall timescale of approx. 3ms, a result that corresponds well with the expected activation time based on the experiment. The analysis is extensive and points out the key interactions and motifs that characterize each state and transition.

Since the recent breakthroughs in experimental structures of mGlu receptors there has been a growth in possible computational studies. This is a good example of using the available structures and a thorough computational approach to probe a question which is beyond the scope of the experiment, namely the full characterization of the activation pathway and its intricate details and intermediates. The work is of value to the field and the wider GPCR research community, it also serves as a fine example of MD and computational simulations used to a high standard to reveal new insights.

The work is well planned and structured. The methods chosen are appropriate, full atom MD methods are needed for the appropriate accuracy and detail to correctly predict the pathway, as this reviewer notes that other smaller scale studies have revealed important cascade effects arising from specific side chain motions and interactions. The large number of computational efforts of the simulations is a requirement, and one should note that the size of the computational system here is very large compared to other simple enzyme systems, in other words, it would have been a major undertaking to run 130 us of simulation. The tICA and MSM work is well performed and appropriate. It represents the state of the art for revealing pathways and kinetic states as required here. The analysis and illustration of the results (figures etc) is well presented. The text is very well written.

The reviewer considers the work to have been performed to a high standard, and there are no apparent doubts or questions regarding data quality etc. The authors have been responsible for similar studies in recent (approx. 5 years) suggesting the work is backed up by extensive experience in the field of computational simulation and interface with biological mechanisms and understanding.
RESPONSE: Thank you for your high affirmation of our work, and your insightful suggestions from drug discovery obviously improved the quality of our manuscript. Following your suggestions, we have carefully revised the manuscript and performed additional simulations to highlight the essential role of allosteric modulators. We hope our detailed responses address your comments.

Recommendations:
The work is complete and publishable in its current form. Here are some suggestions and recommendations:

A key therapeutic approach to modulating mGlu receptor function has small molecule allosteric modulation, indeed mGlu5 receptor NAMs and PAMs have reached clinical trials. Would simulations performed with allosteric modulators in place reveal more insights relevant for drug discovery? If the authors don't consider it necessary to perform simulations with synthetic ligands, it would certainly be of interest to discuss in more detail how the findings of other simulation-based studies, that have used different allosteric modulations. The current work discusses nicely the conformational/activation switches but doesn't venture into commenting on the meaning or validity of how the allosteric modulators interact with those switches, do those hypotheses remain valid?

RESPONSE: We appreciate your thoughtful comments. We totally agree with you that simulations incorporating allosteric modulators could provide crucial insights for drug discovery. However, previous simulation-based studies on allosteric modulators of mGlu5 exhibit two possible limitations: 1) they have concentrated solely on the single 7TM domain, neglecting the substantial extracellular domains and the intrinsic dimeric nature of mGlu5; 2) they employed the NAM-bound mGlu5 structure (PDB ID: 4OO9 or 6FFI) as the initial model to derive the PAM-bound mGlu5 structure through molecular docking, potentially introducing biases due to the distinct mechanisms of action between NAMs and PAMs. Remarkably, recent advancements have been made with the determination of several cryo-EM structures of the full-length mGlu5 receptor in complex with various PAMs in dimeric forms, offering new perspectives on the influence of PAMs on the mGlu5 receptor (Kumar et al., *bioRxiv*, **2023**, 2023.08.29.555158; Cannone et al., *bioRxiv*, **2023**, 2023.11.07.565819). By far, only the structure of mGlu5 complexed with PAM CDPPB has been disclosed (PDB ID: 8TAO). Since the credibility of the initial structure is of vital importance for the subsequent simulations, we tend to explore the significance and validity of the interactions between allosteric modulators and those switches following the release of the structures by Cannone et al.

Moreover, while switches play a crucial role in GPCR activation, the primary focus of our manuscript is the overall model of mGlu5 activation. To further extend our overall model of mGlu5 activation and delve deeper into how the PAM impacts the dynamics of the mGlu5 activation, in the revised manuscript, we leveraged the released cryo-EM structure (PDB ID: 8TAO) to conduct unbiased all-atom MD simulations (1 μs × 10 independent MD simulations) on full-length mGlu5 system, complexed with both the agonist glutamate and PAM CDPPB.

Here, we report our new findings that PAM may enhance mGlu5 activation via conformational bias. Compared to the system where only agonists were added (1 μs × 10 independent MD simulations referencing PDB ID: 6N51), the PAM CDPPB-bound protomer exhibited an outward movement of TM6, decreasing the TM6-TM6 distance and likely leading to a more compact TM6-TM6 interface (Figure S14A). To quantify this, we calculated the interaction free energy between the 7TMs employing the molecular mechanics/generalized Born surface area (MM/GBSA) method. The inclusion of CDPPB significantly strengthens the interaction at the 7TM dimer interface,

with an interaction energy of -16.8 ± 7.3 kcal/mol compared to -2.5 ± 4.9 kcal/mol in the absence of CDPPB (Figure S14B). This result validated a more stabilized active 7TM interface in the presence of CDPPB.

Utilizing Bimane fluorescence, Kumar et al. observed a notable conformational change in the ICL2 upon the addition of CDPPB, distinguishing this effect from that observed with the agonist alone. Although the sensor revealed discrete conformations of ICL2 upon PAM binding, it did not resolve ICL2 structural compositions. Therefore, we generated the FEL of ICL2 from the extensive simulation trajectories (1 μs × 10 repeats × 15 systems). It unveiled that ICL2 existed in a dynamic equilibrium, fluctuating between "closed" or "collapse" states that may occlude the intracellular cavity, and "open" or "extended" states that could facilitate receptor-effector interactions and promote receptor activation (Figure S14C and D). The presence of glutamates alone failed to significantly affect this equilibrium, suggesting that orthosteric agonists by themselves were insufficient to stabilize an active ICL2 conformation. In contrast, the addition of CDPPB, or CDPPB in combination with the G_q protein to the glutamate-bound mGlu5, markedly shifted the equilibrium toward an active ICL2 state, characterized by an appropriately open and extended conformation. Consequently, we proposed that PAM binding transitioned the ICL2 from the inactive closed or collapsed states which might impede the binding of G_q protein, to the active open and extended states which can bind the G_q protein.

These findings collectively demonstrated that PAM CDPPB exerted its positive allosteric modulation effect on mGlu5 by stabilizing not only the active inter-domain 7TM interface but also an appropriately open and extended intra-domain ICL2 conformation. The detailed information has been updated as a supplementary information part (Supplementary Note 6).

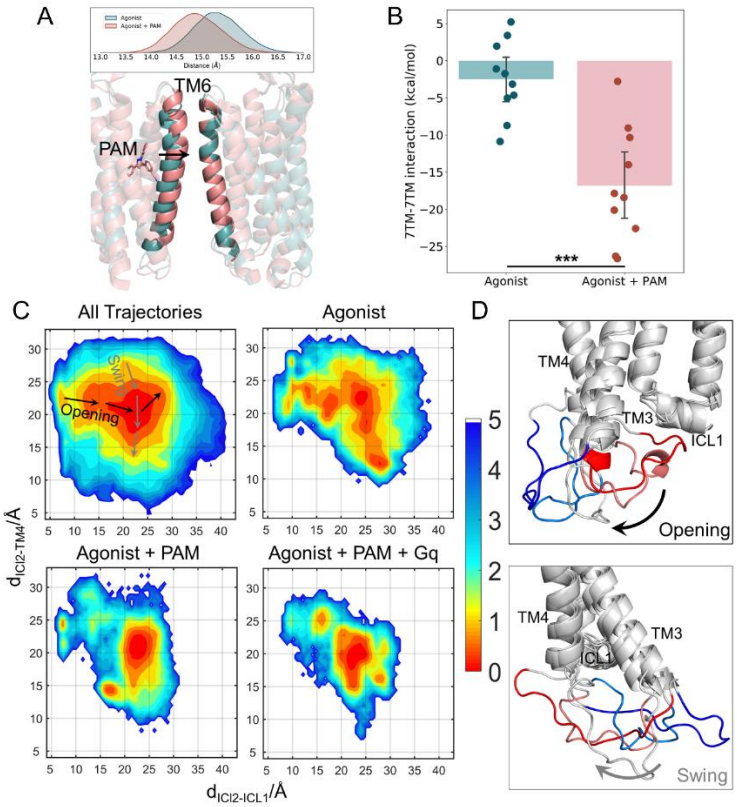

Figure S14. Conformational changes upon CDPPB binding to the mGlu5. (A) The CDPPB, glutamate-bound representative structure (red) exhibits notable proximity trends at the TM6-TM6 interface, as highlighted by the arrow, in comparison to the structure bound with glutamate alone (green). This observation is supported by the quantitative analysis of the distance distribution, specifically measured by the W785$^{6.50}$ Ca-Ca distance. (B) The interaction free energy of the 7TMs (kcal/mol) was calculated using the MM/GBSA method (Reference). The data are presented as mean ± s.e.m. derived from ten independent MD simulations based on the agonist-bound structure (PDB ID: 6N51) and the agonist, PAM-bound structure (PDB ID: 8TAO). Statistical analysis of the differences between these two systems was conducted using a two-way ANOVA, followed by Dunnett's post hoc test ($P < 0.0001$). (C) The conformational landscape of ICL2 derived from simulations. The *x*-axis ($d_{ICL2-ICL1}$) was defined as the distance between the Ca atom of C681 on the ICL2 and the center of mass (COM) of all Ca atoms of ICL1, reflecting the opening motion of ICL2 with increasing $d_{ICL2-ICL1}$ values. The *y*-axis ($d_{ICL2-TM4}$) was determined using the distance between the Ca atoms of C661 on the ICL2 and C691$^{4.30}$ on the TM4, the same points of the fluorescence experiments, representing the swinging motion of ICL2. (D) Representative structures of mGlu5, showcasing the varied conformations of ICL2.

There are some interesting cases in the literature of amino acids that were mutated and shown to be important for mGlu receptor activity, and allosteric activation, however, they were neither located in the orthosteric nor allosteric binding sites. They were in positions 4.51a.41c and 4.52a.42c (and there may be other examples). Are the authors able to rationalize the relevance of these amino acids in their work?

RESPONSE: This is a very enlightening suggestion. As mentioned in our previous response, we would examine these non-orthosteric or non-allosteric but functionally crucial switches in our subsequent work following the release of the structures by Cannone et al.

Make all data and structures available. The input structures and the key intermediate states.
RESPONSE: We have made the input structures, the key intermediate states, and the codes for constructing the Markov State Model (MSM) available at https://github.com/pineappleK/MSM_construction_and_validation.

The accepted IUPHAR/BPS nomenclature for mGlu receptors is to write as mGlu5 receptor, where the 5 is a subscript, not mGlu5 which is a legacy abbreviation. Recommend changing to the new accepted version. https://www.guidetopharmacology.org/GRAC/ObjectDisplayForward?objectId=293
RESPONSE: All the mGlu5 expressions were corrected to the mGlu5 receptor in the revised manuscript. We have also revised the other GPCR names in the manuscript to meet the official name according to the IUPHAR nomenclature.

Reviewer #3 (Remarks to the Author):

The manuscript by Li et al. investigates the challenging problem of mGlu5 dimer activation and reports a Markov State Model (MSM) of based on 130 μs of all-atom MD simulations. A Nudged Elastic Band (NEB) analysis was first performed to generate 13 conformational states that connect the inactive and active states (cryoEM structures). Then, 10 μs of MD simulations were carried out on each state to finally construct the MSM model. I appreciate the approach chosen, which has the potential to yield a comprehensive understanding of this complex system. However, the data at hand are inadequate for assessing the quality of the proposed MSM model, which seems insufficient in describing the intricacies of activation dynamics.

RESPONSE: We are grateful for your constructive critiques, which are vital for enhancing the quality and credibility of our manuscript. Following your suggestions, we meticulously examined the convergence of our NEB procedure, assessed the quality of the MSM, and verified the consistency of our proposed model. We hope our detailed responses address your comments.

There are 3 major concerns:

1. NEB model.

Limited data are provided to ensure the reliability of the simulated transition pathways. While it is difficult to estimate the number of intermediates needed here, one may expect that larger numbers are necessary to describe the conformational changes of such a flexible multi-domain dimer. This naturally comes with higher computational costs for the subsequent MSM model construction. I suggest running NEB calculations with varying numbers of images to assess the convergence and pathway quality.

RESPONSE: We appreciate your insights regarding the convergence of the minimum energy path (MEP) generated by partial NEB. According to your suggestion, we conducted a convergence test by altering the number of interpolated images (i.e., 16, 24, 32 and 40). The results demonstrated that employing 16 images yielded sporadic coverage of the transition pathway, whereas using more than 24 images ensured a more complete and consistent exploration (Figure S1). Our findings suggested that 32 images might offer an optimal compromise between computational efficiency and thorough pathway investigation.

Furthermore, we conducted a systematic survey of the literature on the application of the NEB technique in biomolecular simulations. Representative studies involving monomeric proteins (Li et al., *ACS Chem Biol*, **2014**, 9(4):986-993; Lu et al., *Nat Commun.*, **2021**, 12(1):4721), polymeric proteins (Dodd et al., *Nat Commun*, **2020**, 11(1):5379; Fallon et al., *J Am Chem Soc*, **2021**, 143(30):11349-11360), and protein-DNA systems (Li et al., *J Am Chem Soc*, **2017**, 139(7):2682-2692; Bergonzo et al., *J Am Chem Soc*, **2011**, 133(37):14504-14506). All these studies preferred using between 22 and 32 images for exploring the MEP, successfully generating a reliable MEP for subsequent mechanism investigations, even for full-length, SARS-CoV-2 spike glycoprotein ectodomain, a much more flexible and complex multi-domain trimer.

Therefore, our choice of 32 images for investigating the activation pathway of the dimeric mGlu5 receptor is both sufficient and well-supported by existing research practices. We hope that the convergence test for the partial NEB presented here will assist other researchers in verifying and establishing a reliable transition pathway. The detailed information has been updated as a supplementary information part (Supplementary Note 1).

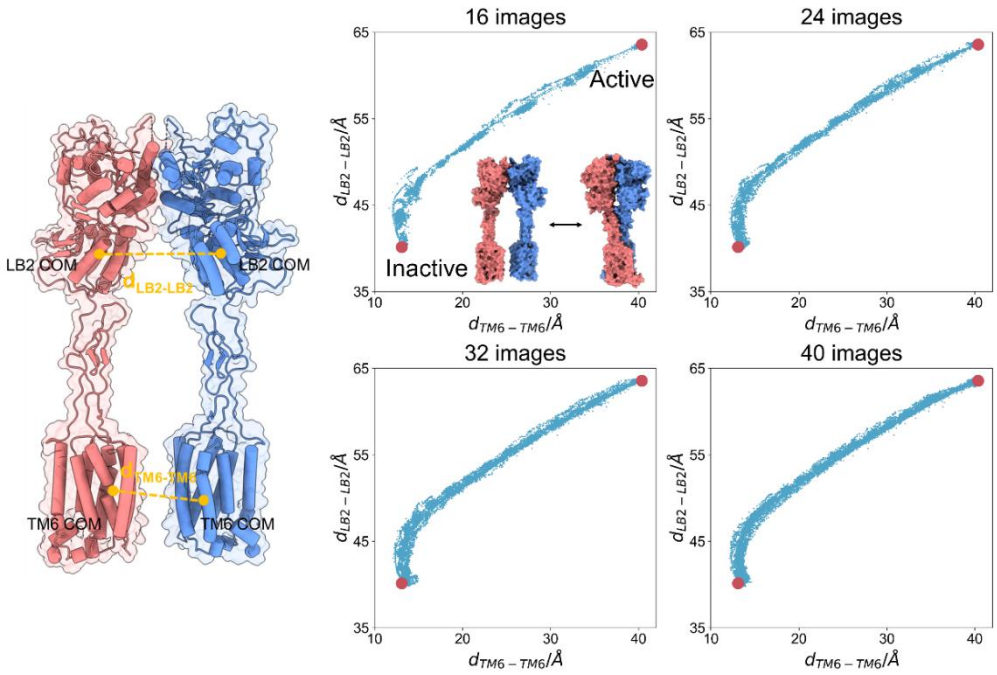

Figure S1. Partial NEB calculations were conducted in explicitly solvated systems using 16, 24, 32, and 40 images to examine the convergence of the transition pathway. In each panel, the red circles are the endpoints of the cryo-EM structures of mGlu5 while blue circles represent simulation snapshots captured at intervals of 10ps.

2. MSM model.

The choice of the MSM hyperparameters (e.g., 2 tICs, 300 microstates and 1 ns lag time) is unjustified. This makes it difficult to evaluate the model's quality. Given the complexity and slow dynamics of the system, 2 tICs and 1 ns lag time are probably insufficient. The author may use variational approach for Markov processes (VAMP2) or Generalized matrix Rayleigh quotient (GMRQ) scores in a cross validation to determine the numbers of tICs and microstates required. An example can be found in Westerlund et al. Plos Comput Biol 2022.

The tICA was performed on "the coordinates of Cα of mGlu5". More details are necessary about how the tICA was performed and why 2 tICs were used for the MSM. Therefore, although the ITS validation in Fig S1 appears satisfying (which timestep is used?), 2 tICs and 1 ns lag time are likely too short for a system with both fast and slow dynamics.

RESPONSE: Thanks for your professional suggestions for constructing a high-quality MSM. Following your suggestions and the protocol by Westerlund et al. (*PLoS Comput Biol*, **2022**, 18(10):e1010583), our procedures to construct and validate MSM have been

highly improved in the following four aspects, and the MSM results were justified:

(1) For tICA projection, we first removed the translational and rotational motions that did not contribute to the intrinsic dynamics of the system, which was accomplished by performing a coordinate RMS best-fit to the averaged coordinates of the trajectories. Subsequently, all MD trajectories were featurized into a vector space with the aligned Cα cartesian coordinates of mGlu5. The high-dimensional vector space was dimensionally reduced using tICA with a lag time of 10 ns.

(2) For the MSM hyperparameter selection, we calculated the GMRQ scores at varying numbers of tICs and microstates via 5-fold cross-validation. As shown in Figure S2A, the choice of 2 slowest tICs and 300 microstates was sufficient to describe the MSM. The inclusion of more than 5 tICs and 500 microstates could lead to overfitting. Hence, the 2 slowest tICs were clustered into 300 microstates by the K-means algorithm.

(3) To select a memoryless lag time, we performed the implied timescale test. The implied timescales appeared to be coverage from a lag time than 5 ns (Figure S2B). To guarantee the accuracy of our analysis, we set 10 ns as the lag time of our system.

(4) For macrostate classification, the 300 microstates were further clustered into 5 macrostates through the PCCA+ algorithm. The 5 macrostates were well separated on the tICA landscape (Figure S2C) and validated by the Chapman-Kolmogorov test (Figure S2D).

Thereafter, the updated MSM hyperparameters (Old: 2 tICs, 300 microstates and 1 ns lag time; New: 2 tICs, 300 microstates and 10 ns lag time) were justified, leading to an inter-subunit rearrangement time estimation of 0.99 ms (Old: 3.54 ms) which is still comparable to the ~1-2 ms inter-subunit activation timescale in the mGluR1 homodimer (Grushevskyi et al., *Proc Natl Acad Sci U S A*, **2019**, 116(20):10150-10155). Your concerns about this timescale will be replied in your following comment *3c*. The detailed information has been updated as a supplementary information part (Supplementary Note 2). Thank you.

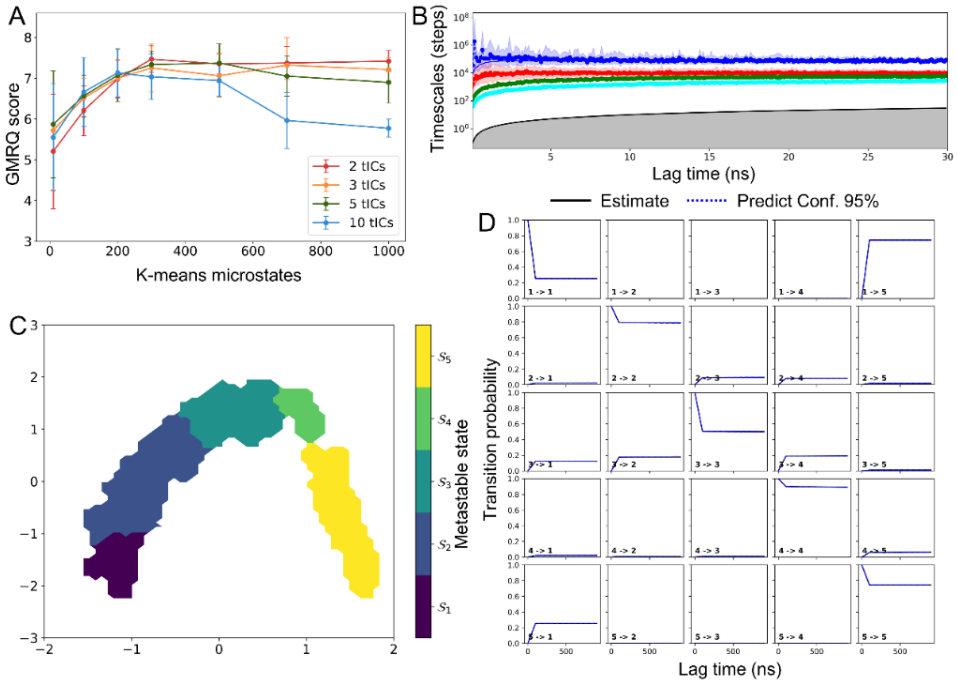

Figure S2. The validation of an MSM constructed by tICA. (A) The optimization of MSM hyperparameters by calculating GMRQ scores at varying numbers of tICs and microstates. The mean GMRQ scores from 5-fold cross-validation are plotted as dots and standard deviations are plotted as error bars. (B) The results of the implied timescale test. Four distinct resolved timescales colored in blue, red, green, and cyan lines are shown as a function of lag time. The 95% confidence intervals for the eigenvalues are depicted as shaded areas. A black solid curve marks the boundary of a shaded region, indicating where the implied timescales fall short of the lag time. (C) The distribution of 5 macrostates on the landscape. Corresponding colors are shown on the right. (D) The results of the 5-state Chapman-Kolmogorov test. The probabilities of transiting between the macrostates (dash lines) observed in the simulations are consistent with the estimated probabilities from the constructed MSM (solid line).

3. Experimental validation

a. I acknowledge that the authors performed site-directed mutagenesis to examine 4 microswitches in sensitive regions. Although microswitches are an important aspect of GPCR activation, the primary issue with the manuscript is the credibility of the overall model of mGlu5 activation. A preprint posted by the Kobilka lab in August (Kumar et al., *bioRxiv*, **2023**, 2023.08.29.555158) has captured several intermediate states by cryoEM/smFRET that illustrate the stepwise activation. A more recent preprint describes similar intermediate states even for PAM-bound structures (Cannone et al., *bioRxiv*, **2023**, 2023.11.07.565819). The intermediate-state structures are available for comparison with the models proposed in this manuscript.

RESPONSE: We totally agree with your suggestions. Kumar et al. have released four cryo-EM structures of mGlu5, including **Quis-bound intermediate 1a** (PDB ID: 8T7H), **Quis-bound intermediate 2a** (PDB ID: 8T8M), **Quis and CDPPB-bound intermediate 3a** (PDB ID: 8TAO), and **CDPPB-bound inactive intermediate 1b** (PDB ID: 8T6J). Although Cannone et al. have not released their structures, we can still make the comparison through their article. Next, let us compare the recently determined intermediate-state structures with our proposed models one by one.

(1) **Quis-bound Intermediate 1a:** The Intermediate 1a exhibits an Rcc conformation, characterized by two closed VFTs domains while the CRDs and 7TMs remain as far apart as in the inactive mGlu5 state. In alignment with this, our in-depth analysis of the S2 metastable state identified an alternative configuration of the VFTs (denoted as S2', minimal Cα RMSD to Intermediate 1a: 3.8 Å), in which the VFT of protomer A transitioned from an open (S2, Rco) to a nearly closed state ($RMSD_{VFT}^{A}$ = 1.8 Å), closely approaching a Rcc conformation (Figure 3B). Moreover, Cannone et al. have captured a transient and non-classic binding pose of quisqualate (a glutamate analogue) in the Rcc conformation of mGlu5. Similarly, our simulations also captured the dynamic binding poses of glutamate, particularly within the S2 state (Figure S4), highlighting the substantial flexibility of the VFT domains. We have added the comparison in the revised manuscript accordingly throughout the text and figures (Figure 3 and Supplementary Note 4)

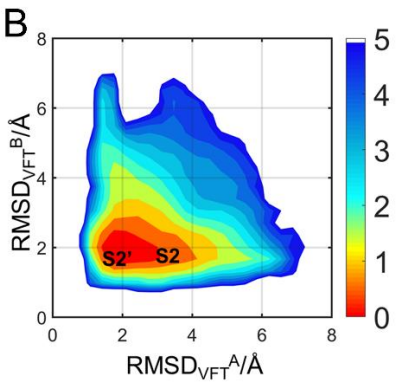

Figure 3B. A per-protomer analysis of the S2 metastable state uncovered an alternative configuration of the VFTs, termed S2'.

(2) **Quis-bound Intermediate 2a:** The Intermediate 2a, simultaneously stabilized by Quis and Nb43 exhibits a conformation remarkably similar (Cα RMSD = 2.3 Å) to the structure of 6N51 (also complexed with Quis and Nb43) determined by the Kobilka lab in 2019. Both structures are identified within the S5 through our simulations (minimal Cα RMSD = 2.2 Å).

Significantly, our simulations uncovered two additional metastable states, S3 and S4, which might bridge the Intermediate 1a and 2a. These transient metastable states may prove challenging to stabilize by cryo-EM. In these metastable states, we revealed the role of the B2' module in mediating the active CRDs interface. This active CRDs interface was confirmed by introducing a cysteine-mediated crosslink at the potential interface of the B2' module (I523C). As shown by the replotted Figure 4C and D, the I523C mutant maintained comparable levels of cell surface expression but demonstrated a robust constitutive activity as high as the glutamate-induced activity in the wild type (WT). Mutating the I523 residue to alanine (I523A) or altering its adjacent two residues (K521&V522&I523A, I523&R524&K525A) led to the absence of constitutive activity and a significant reduction in efficacy, yet cell surface expression levels remained similar to those of the WT. We have added these results in the revised main text.

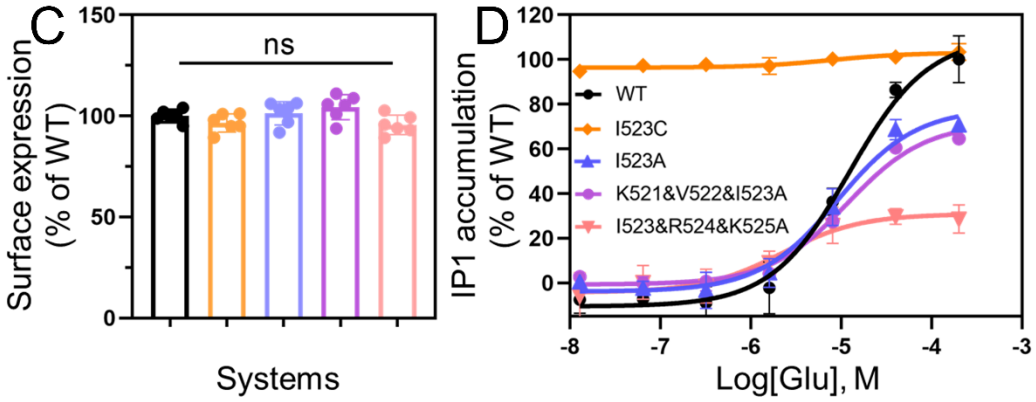

Figure 4. Experimental verification of the observed CRD association dynamics. (C) Quantification of cell surface expression. Data are presented as mean ± s.e.m. of six independent experiments. ns, not statistically significant (one-way ANOVA with

Dunnett's post hoc test). (D) Crosslinking at the potential surface of the B2' module by an I523C mutant displays high constitutive activity, as measured using IP accumulation. Alanine mutation of critical residues involved in forming the observed B2'-mediated interface blunt glutamate-induced signaling compared to the WT. Data are presented as mean ± s.e.m. of three independent experiments.

(3) **Quis and CDPPB-bound Intermediate 3a:** Kumar et al. observed an asymmetric TM6-TM6 interface in Intermediate 3a, highlighting the critical asymmetric microswitch $Y799^{6.44}$. These asymmetric features, although absent in earlier apo (PDB ID: 6N52) and active (PDB ID: 6N51) mGlu5 structures that are endpoints of our simulations, have been successfully captured in our extensive simulations. The critical role of $Y799^{6.44}$ in receptor activation has been confirmed through our site-directed mutagenesis experiments (Figure 5).

In addition, Kumar et al. failed to determine the ICL2 conformation in the cryo-EM structure of Intermediate 3a. Utilizing Bimane fluorescence, they observed a notable conformational change in the ICL2 upon the addition of CDPPB, distinguishing this effect from that observed with the agonist alone. Although the sensor revealed discrete conformations of ICL2 upon PAM binding, it did not resolve ICL2 structural compositions. To delve deeper into how the PAM impacts the dynamics of the mGlu5 activation and further extend our model of mGlu5 activation, leveraging the cryo-EM structure (Intermediate 3a), we conducted unbiased all-atom MD simulations (1 μs × 10 independent MD simulations) on full-length mGlu5 system bound with agonist glutamate and PAM CDPPB. Combined with the prior extensive simulation trajectories (1 μs × 10 × 13 NEB replicas), we generated the conformational landscape of ICL2 (Figure S14 C and D). It unveiled that ICL2 existed in a dynamic equilibrium, fluctuating between "closed" or "collapse" states that may occlude the intracellular cavity, and "open" or "extended" states that could facilitate receptor-effector interactions and promote receptor activation. The presence of glutamates alone failed to significantly affect this equilibrium, suggesting that orthosteric agonists by themselves were insufficient to stabilize an active ICL2 conformation. In contrast, the addition of CDPPB to the glutamate-bound mGlu5 markedly shifted the equilibrium toward an active ICL2 state, characterized by an appropriately open and extended conformation. Consequently, we proposed that PAM binding transitioned the ICL2 from inactive closed or collapsed states which might impede the binding of G_q protein, to the active open and extended states which can bind the G_q protein. The detailed information has been updated as a supplementary information part (Supplementary Note 6).

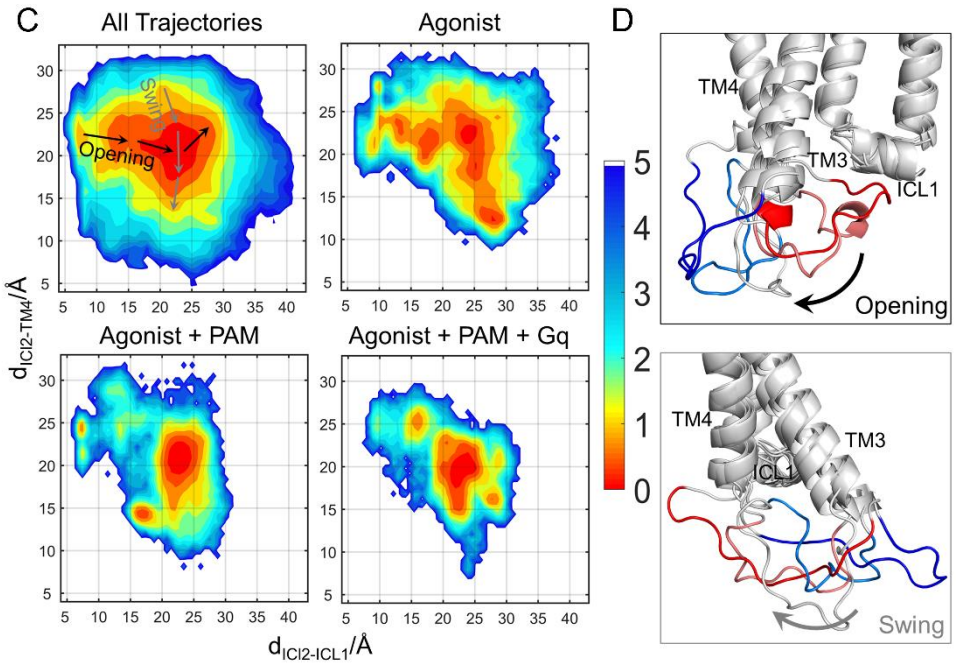

Figure S14. Conformational changes upon CDPPB binding to the mGlu5. (C) The conformational landscape of ICL2 derived from simulations. The *x*-axis ($d_{ICL2\text{-}ICL1}$) was defined as the distance between the Ca atom of C681 on the ICL2 and the center of mass (COM) of all Ca atoms of ICL1, reflecting the opening motion of ICL2 with increasing $d_{ICL2\text{-}ICL1}$ values. The *y*-axis ($d_{ICL2\text{-}TM4}$) was determined using the distance between the Ca atoms of C661 on the ICL2 and C691$^{4.30}$ on the TM4, the same points of the fluorescence experiments, representing the swinging motion of ICL2. (D) Representative structures of mGlu5, showcasing the varied conformations of ICL2.

(4) **CDPPB-bound inactive Intermediate 1b:** Although Intermediate 1b is beyond the scope of our research, it inadvertently validated the moderate inter-domain dynamics within the CRDs, even when mGlu5 is inactive, as demonstrated in our simulations (Figure S8). The profiling of CRDs inter-domain dynamics—quantified by the distance between residues D560 across both protomers—revealed that, even in the inactive state, 97% of the conformations can fluctuate from 68.0 Å to 78.0 Å. In the apo inactive cryo-EM structure, the distance is 68.3 Å (PDB ID: 6N52). In the antagonist-bound inactive cryo-EM structure, the distance is 70.2 Å (PDB ID: 7FD9) (Nasrallah et al., *Cell Rep*, **2021**, 36(9):109648). In the Intermediate 1b (PDB ID: 8T6J), the distance is 73.4 Å, which is close to the metastable state S1 (74.3 Å). This variability highlights the inherent flexibility within the CRDs, even in states traditionally considered inactive.

b. In particular, activation of the ECD appears uncoupled (or loosely coupled) to that of the 7TM. This does not seem to be the case here.

RESPONSE: Thanks for this important comment. The activation of the ECDs and 7TM domains are loosely coupled in our simulations. It is widely recognized that in monomeric β2-adrenergic receptor, the ligand-binding site is loosely coupled to the

connector, which in turn is loosely coupled to the G-protein-binding site (Manglik et al., *Cell*, **2015**, 161(5):1101-1111; Dror et al., *Proc Natl Acad Sci U S A*, **2011**, 108(46):18684-18689). Similar loose couplings were observed in the dimeric, multidomain mGlu2 receptor between the VFT domains (ligand-binding site) and the CRDs (connector), as evidenced by smFRET spectroscopy (Liauw et al., *Nat Chem Biol*, **2021**, 17(3):291-297). Our simulations extended these observations by revealing loosely coupled dynamics not only between the VFT domains and CRDs (R2 = 0.62) but also between the CRDs and the 7TM domains (G-protein-binding site, R2 = 0.58). This contrasted with the tighter coupling observed between the VFT and the B2' module of CRDs (R2 = 0.91), which are linked by inter-domain disulfide bonds. The three functionally relevant regions of mGlu5—the VFT domains, CRDs, and the 7TM domains—appear to be loosely coupled to one another. These results suggested that such loose coupling could represent a general mechanism of allosteric regulation across both monomeric and dimeric GPCRs. The detailed information has been updated as a supplementary information part (Supplementary Note 3).

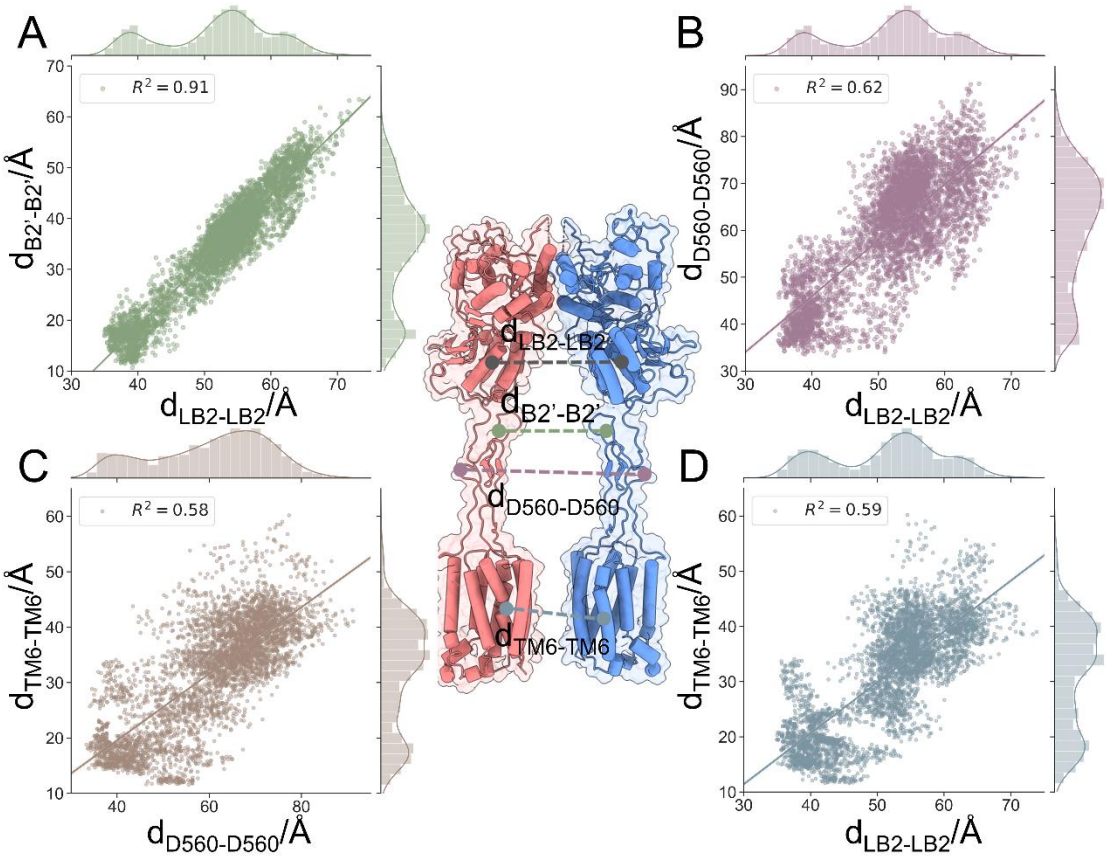

Figure S3. Inter-protomer motion correlation between two functional relevant domains. The results include correlations between the VFT and the B2' module of CRDs (A), the VFT and the second A1 module of CRDs (B), the second A1 module of CRDs and the 7TM (C), the VFT and 7TM domains (D). The inter-protomer dynamics between the VFT, the B2' module, the second A1 module of CRDs, and the 7TM domains are quantified by measuring the distance distributions between LB2-LB2 COM, B2'-B2' COM, D560-D560 Cα and TM6-TM6 COM, respectively. Scatter points represent simulation snapshots taken at 20ns intervals.

c. Concerning the activation kinetics, the MSM model here suggests a timescale of ~2 ms which "is in agreement with the experimentally validated activation timescale of 1–2 ms for the mGluR1 homodimer" (p. 7, l. 177-179). Several questions arise from this statement:

- the 2 ms timescale in the mGluR1 study (M. Lohse lab 2019) referred to the intramolecular motions of the 2 protomers, whereas the activation of the 7TM was much slower (~ 20 ms). The latter is presumably associated with G protein coupling, beyond the scope of this manuscript. However, the 2 processes should be specified to avoid confusion. The preprint from the Kobilka lab has shown that 7TM undergoes further conformational changes in the presence of G proteins (unlike mGluR2). Therefore, mGlu5 activation within 7TM also involves 2 processes, the intramolecular motions (protomer approximation) and intramolecular TM conformational changes triggered by G protein binding.

RESPONSE: We agree that the 1-2 ms timescale in the mGluR1 study referred to the intramolecular motions of the 2 protomers, corresponding to the inter-subunit conformational arrangement. To avoid confusion, we have thus removed the "activation timescale" expression in the revised manuscript and used "inter-subunit rearrangement timescale" instead:

"It was shown that the initial inter-subunit rearrangement between the mGlu5 subunits occurred within approximately 1 ms. This observation is consistent with the recently experimentally validated inter-subunit rearrangement timescale of 1–2 ms in the mGlu1 homodimer."

- in the case of mGluR2 (Olofsson et al. Nat Commun 2014), merely the ECD dimer activation takes > 4 ms. The full-length dimer activation may be even slower. Different mGluR subtypes show different apo states and conformational changes upon activation. It is highly speculative to assume the same activation timescales for different mGluRs.

RESPONSE: Thank you for your questions. Olofsson et al. showed that a majority of receptor ECD dimers oscillate on a 50–100 µs timescale between the two main conformations, attributed to the resting and the active state of the receptor. The exclusive role of ligands is to modulate the transition rates between these states. Only a small fraction of ECD dimers appear locked in the R or the A state for periods exceeding 4 ms. Moreover, they proved that besides mGlu2 (class II mGlu), mGlu4 (class III mGlu) and mGlu5 (class I mGlu) exhibited surprisingly the same fast structural dynamics, on a sub-millisecond timescale, corresponding to transitions between an activated and a resting state. It means that glutamate binding could module the ECD dimers of mGlu5 from the resting state to the activated state on a sub-millisecond timescale, not over 4 ms.

We agree with you that caution is warranted in assuming that mGlu5 undergoes a similar full-length dimer activation process as other mGlu receptors, given that different classes of mGlu receptors share only 45% sequence identity. However, within class I mGlu receptors, mGlu5 stands out as the sole evolutionary counterpart with mGlu1, sharing a 70% sequence similarity. This significant similarity suggests a potential for

mGlu5 and mGlu1 to share comparable inter-subunit conformational arrangement timescales. It's important to note, though, that Olofsson et al. conducted validations only on mGlu2, mGlu4, and mGlu5. Despite this, they extended their conclusion to all mGlu subtypes, justifying this by pointing out the approximately 70% sequence identity among receptors within the same group.

We totally understand your concerns, so we have meticulously revised our wording to highlight the subtle differences between mGlu1 and mGlu5 for readers:
"*Given that mGlu1 shares roughly 70% sequence similarity with mGlu5 and the two receptors represent the evolutionary counterparts among the class I mGlu receptors, this consistency strongly confirmed the precision and reliability of our computational methodology in capturing the dynamics of mGlu5 activation.*"

While this work holds promise, a substantial volume of additional simulations and analyses are necessary to achieve a convincing MSM model. Only then can one evaluate the results and discussions on the detailed motions and microswitches. I regret that the manuscript in its current form does not meet the standards required for publication in Nat Commun.

RESPONSE: Thank you for the constructive critiques you have provided. Let us address the points you have raised as follows:

Firstly, the concern about the convergence of NEB pathways. Following your suggestions, we have incorporated a convergence test at varying images to ensure the quality of NEB pathways.

Secondly, we appreciate the raised issue regarding the MSM. As per your suggestions, the GMRQ scores at varying numbers of tICs and microstates via 5-fold cross-validation were calculated to determine the optimal hyperparameters. The credibility of memoryless lag time and macrostate classification was further confirmed by the implied timescale test and Chapman-Kolmogorov test.

Thirdly, the validity of our mGlu5 activation model was further reinforced by the newly available cryo-EM structures. Moreover, our dynamic simulation-based novel insights beyond the static cryo-EM structures are also highlighted.

We have tried our best to address all the concerns by providing further explanations and supplying experiments, which substantially improve the quality of our work. Thank you.

Reviewer #4 (Remarks to the Author):

The purpose of the study from Li et al. is to provide insights into the activation mechanism of mGlu5 receptor, a homodimer complex belonging to class C family of G-protein coupled receptors. More precisely, the authors wish to describe the transition states and timescale along the conformational landscape of the activation process. It may be that the modeling approach allows to capture transition states that are not stable enough to be captured by structural or biophysical methods.

The manuscript relies on predictive modeling of intermediate states between the resting and active conformations of mGlu5 receptor homodimer. For the starting and final conformations, the authors used the coordinates of two cryo-EM structures described in Koehl et al. Nature 2019 (PDB ID 6N52 and 6N51). A major challenge is to comprehend a process that occurs on a millisecond scale when molecular modeling is usually limited to microsecond events.
The authors first defined the minimum energy path (MEP) between the resting and active states of full-length mGlu5 receptor. Then molecular dynamics (MD) simulations in explicit solvent models were run for 13 conformations identified at the previous step and distributed along the activation pathway. Next, time-structure-based independent component analysis (tICA) was applied to the MD trajectories and allowed the identification of five metastable states S1 to S5. Representative conformations of these 5 states along the transition pathway from Resting to Active agonist bound, are then thoroughly analyzed in a large part of the manuscript.
RESPONSE: We are grateful for your constructive critiques, which are vital for enhancing the clarity and quality of our manuscript. We hope our detailed responses address your comments.

Comments

1) Five sequential metastable states S1 to S5 were identified along the activation pathway of mGlu5 receptor. Representative structures of these five states were then characterized.
S1 and S5, represent the initial and last conformations of the activation process, corresponding to the inactive and active agonist bound cryo-EM structures (PDB ID 6N52 and 6N51). Thus, the interest is in the S2, S3 and S4 intermediate conformations and the kinetics of the whole activation pathway.
The authors first describe the changes of the whole dimer and kinetics aspects. They observe an asymmetrical dimer arrangement in 200µs between S1 and S2, a rate-limiting step of 2.14 ms to reach S4 and a total of 3.54 ms from S1 to S5 when activation is initiated by glutamate binding. They claim that a similar time scale has been experimentally observed by Olofsson et al. (ref 39) for the VFT domain and by Grushevskyi et al. (ref 35) for the whole pathway. Although the sub-milliseconds of the VFT activation are indeed well known since the work of Olofsson et al. in 2014, it is more questionable for the whole pathway to the active agonist bound state. For mGlu1

receptor, Grushevskyi et al. identified two metastable intermediate states that are reached in sub-milliseconds for the first one and 1 ms for the second but it takes about 20 ms to switch to the fully active conformation. Rondard and Pin (Rondard et al., *Curr Opin Pharmacol*, **2015**, 20:95-101) when summarizing several studies, mention 35 ms to get to the second metastable state (a conformation with a first relative rearrangement of the two 7TMs) and 50 ms for the full activation. Recent studies show that interaction with the G-protein (which happens in cells) in the fully active state extends the timescale for full activation. Yet the authors of the present manuscript should give more support to the rather short time between S1 and S5 that they calculated.

RESPONSE: We appreciate your questions regarding our whole agonist-indued activation kinetics. It is well known that the mGlu receptors undergo sequential inter- and intra-subunit conformational rearrangements during activation. Our kinetic MSM was constructed on the whole aligned Cα coordinates, primarily capturing the inter-subunit dynamics of mGlu5. We reference the similar timescale identified by Grushevskyi et al. (We would explain the reasons we cited their works in the subsequent paragraph) to reinforce the credibility of our MSM with biological observations, complementing the model's mathematical validation through the rigorous implied timescale test and the Chapman-Kolmogorov test.

We agree with you that the intra-subunit activation is presumably associated with G protein coupling, which extends beyond the scope of our original manuscript. However, in the revised version, we tried to provide further mechanistic insights into G protein coupling to address your comment *4c*. To avoid confusion, we meticulously changed the expression as follows:

"It was shown that the initial inter-subunit rearrangement between the mGlu5 subunits occurred within approximately 1 ms. This observation is consistent with the recently experimentally validated inter-subunit rearrangement timescale of 1–2 ms in the mGlu1 homodimer. Given that mGlu1 shares roughly 70% sequence similarity with mGlu5 and the two receptors represent the evolutionary counterparts among the class I mGlu receptors, this consistency strongly confirmed the precision and reliability of our computational methodology in capturing the dynamics of mGlu5 activation."

Here are the reasons we cited the works by Grushevskyi et al. To the best of our knowledge, there have been three studies aimed at uncovering the fast activation inter-subunit timescale of mGlu1. Rondard and Pin (Rondard et al., *Curr Opin Pharmacol*, **2015**, 20:95-101) reviewed an approximately 35 ms timescale, which originated from the works of Hlavackova et al. (Hlavackova et al., *Sci Signal*, **2012**, 5(237):ra59), who utilized a superfusion device. Prior to this, Marcaggi et al. identified an upper limit timescale of 10 ms through specifically designed experiments to monitor rapid effects (Marcaggi et al., *Proc Natl Acad Sci U S A*, **2009**, 106(27):11388-11393). In 2019, Grushevskyi et al. employed finer submillisecond FRET recordings using two distinct methods: 1) UV light-triggered uncaging of glutamate in intact cells and 2) piezo-driven solution exchange in outside-out patches, to determine the 1–2 ms inter-subunit activation timescale of the mGlu1. These prompted us to cite their work in our study.

2) Then the authors detailed the fold of protomer A and B in the different states.

For the first state S1, they find both protomers holding an open VFT and a dimer conformation close to the 6N52 structure. Quisqualate had been replaced by glutamate which binds to the upper lobe of the VFT. Surprisingly, the α-carboxylate of glutamate is not binding to the conserved Ser152 and Thr175 of the upper lobe as in the X-ray structure 1EWK:B. These two residues are bound to the α-carboxylate of agonists/antagonists in all VFT structures, open or closed. See for example mGlu1 VFT bound to LY341495 or to MCPG in 3KS9 and 1ISS respectively. In these structures the γ-carboxylate interacts with a conserved Lys and Tyr in group I of mGluRs (K409/K396 and Y74/Y64 in mGlu1 and mGlu5 respectively). Lys409/Lys396 is a conserved Lys all through the 8 mGlu receptors and always makes a salt bridge with the γ-carboxylate of agonists/antagonists deriving from glutamate. Thus in the first S1 conformation, the docking of glutamate is inverted (Figure S3). This wrong initial docking must have major consequences in the other conformations. Indeed in the following state S2 (Figure S4) the α-carboxylate of glutamate makes salt bridges with Lys396, Arg68 (protomer A) and Arg310 (protomer B) which are well known to interact with the γ-carboxylate. This inversion of glutamate and derivatives is quite common when carrying out dockings and one should be careful in choosing the poses. In the S3 state, the classical docking is recovered with the α-carboxylate of glutamate making H-bonds with Ser52 and Thr173. Thus S1 and S2 conformations bound to glutamate are questionable. In particular it is strange that glutamate bound to the closed protomer B of state 2 twists around in S3. The authors should check their dockings and if they confirm the S1 and S2 dockings explain why they do not comply with all published structures and 3D-models.

RESPONSE: Thank you for this important comment. The "inverted" glutamate binding modes observed in S1 and S2 were elucidated through extensive MD simulations, not as a result of artificial selection from multiple molecular docking outcomes. Molecular docking was employed solely during the initial system preparation using structures from 6N52 and 6N51 (PDB ID). Throughout this preparation phase, all potential binding poses were carefully evaluated, considering not only the predicted binding free energy but also the conservation of key interactions, as you commented. Most of the conserved interactions (e.g., interactions between the α-carboxylate of glutamate and the conserved Ser152 and Thr175, and its γ-carboxylate with Y64 and K396) were included after preparation (Figure R2).

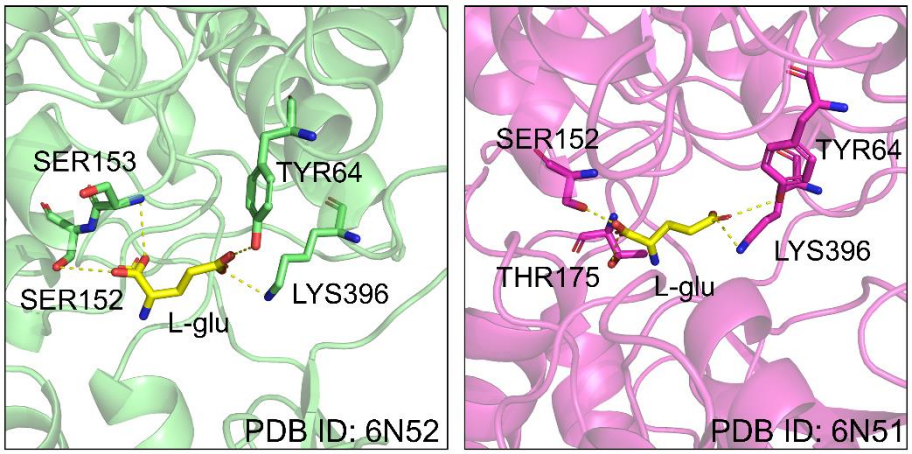

Figure R2. Initial glutamate docking poses in the inactive (6N52) and active structures (6N51). Only protomer A is shown, as it maintains the same pose as protomer B.

Thereafter, large-scale MD simulations were performed to stimulate the glutamate-induced mGlu5 activation. One MD simulation study of drug binding to GPCRs has noticed that drugs can initially bind in non-crystallographic poses before transitioning to crystallographic poses (Dror et al., *Proc Natl Acad Sci U S A*, **2011**, 108(32):13118-13123). Similar dynamic behavior has also been observed for glutamate binding. It can assume the non-crystallographic, inverted poses in various glutamate-binding systems, including the ionotropic glutamate receptors (i.e., GluA2 of the AMPA receptor and GluN2A of the NMDA receptors (Yu et al., *Neuron*, **2018**, 97(1):139-149.e4; Yu et al., *Structure*, **2018**, 26(7):1035-1043.e2)), and periplasmic binding proteins (i.e., ligand-bound glutamine binding protein (Zhang et al., *Commun Biol*, **2020**, 3(1):419)). Very recently, Cannone et al. discovered an intermediate and transient binding pose of quisqualate (a glutamate analogue) in a mGlu5 cryo-EM structure. The quisqualate was found to only form polar interactions with D305 and S173, diverging from the classical binding pose, which typically involves polar interactions with the conserved residues Y64, S152, T175, and K396.

Consistently, our simulations further revealed that glutamate could initially bind in a transient, non-crystallographic pose, eventually transitioning to the crystallographic pose in mGlu5. In the initial S1 state, glutamate's binding pose was inverted. In protomer A, the α-carboxylate of glutamate interacted with the side chains of R68, S173 and K396, whereas its γ-carboxylate interacted with the side chains of S42, W100 and S151. In protomer B, its α-carboxylate made polar contacts with the side chains of R68 and K396, while the γ-carboxylate contacted the side chains of Q46 and R61. This inverted binding was partially maintained in the subsequent S2 state, where the α-carboxylate of glutamate contacted the side chains of R68 and K396 in protomer A and R310 in protomer B, interactions typically formed with the γ-carboxylate in the available crystallographic structures. Eventually, the glutamate began to adopt the classic binding mode, with its α-carboxylate coordinating with S152 and T175 and γ-carboxylate forming polar contacts with Y64 and K396 (in S2') and R310 (in S3).

These observations from our simulations, in conjunction with data from prior studies, do not contradict the energetically favorable classical crystallographic binding modes of glutamate. Rather, it simply suggests the possibility of an alternative or dynamic binding pose, which also indicates a significant degree of dynamic within the VFT domains. The detailed information has been updated as a supplementary information part (Supplementary Note 4).

3) A paragraph is focused on the analysis of the CRD domains that link the VFT and 7TM domains in each protomer. The authors found that the CRD module bound to the VFT displays more flexibility than the module linked to the 7TM as previously observed (see for example Liauw et al. Nat Chem Biol 2021 demonstrating "VFT and CRD domains loosely coupled"). It is not clear which of the intra-domain CRD conformations observed during the simulations (Figure 4) are found in which of the S1

to S5 states. Regarding the inter-domain conformational arrangement of the CRDs, the elaborated study from Liauw et al (Nat Chem Biol 2021) defined four states that are claimed to coincide with S1 to S4 of the present study. However there seems to be a discrepancy in particular the S1 state in Figure S8 does not seem to correspond to the initial symmetrical resting conformation. This needs to be clarified. To support their results, the authors introduced some mutations from Arg524 to Trp532 and performed functional assays but they did not enumerate in what residues they were mutated into. This needs to be added and interpreted according to the mutations.

RESPONSE: Thanks for your questions. Let us answer them one by one.

(1) The authors found that the CRD module bound to the VFT displays more flexibility than the module linked to the 7TM as previously observed (see for example Liauw et al. Nat Chem Biol 2021 demonstrating "VFT and CRD domains loosely coupled").

Our findings showed that the CRD module bound to the VFT (B2' module) displayed more flexibility than the module linked to the 7TM (the second A1 module), describing the intra-domain dynamics within the CRD. In contrast, Liauw et al. (Liauw et al., *Nat Chem Biol*, **2021**, 17(3):291-297) investigated the inter-domain dynamics of CRDs, focusing on residue D560 using smFRET spectroscopy. Their results only suggested that the VFT domains are loosely coupled with the CRDs.

It is widely recognized that in monomeric β_2-adrenergic receptor, the ligand-binding site is loosely coupled to the connector, which in turn is loosely coupled to the G-protein-binding site (Manglik et al., *Cell*, **2015**, 161(5):1101-1111; Dror et al., *Proc Natl Acad Sci U S A*, **2011**, 108(46):18684-18689). Our simulations extended these observations by revealing loosely coupled dynamics not only between the VFT domains and CRDs (R2 = 0.62) but also between the CRDs and the 7TM domains (G-protein-binding site, R2 = 0.58). This contrasted with the tighter coupling observed between the VFT and the B2' module of CRDs (R2 = 0.91), which are linked by inter-domain disulfide bonds. The three functionally relevant regions of mGlu5—the VFT domains, CRDs, and the 7TM domains—appear to be loosely coupled to one another. These results suggested that such loose coupling could represent a general mechanism of allosteric regulation across both monomeric and dimeric GPCRs. The detailed information has been updated as a supplementary information part (Supplementary Note 3).

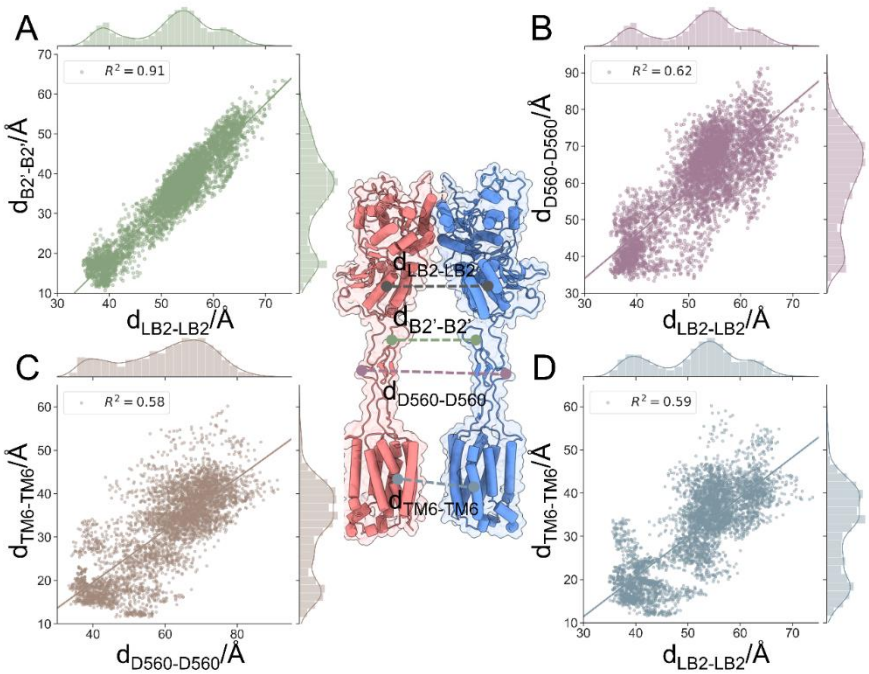

Figure S3. Inter-protomer motion correlation between two functional relevant domains. The results include correlations between the VFT and the B2' module of CRDs (A), the VFT and the second A1 module of CRDs (B), the second A1 module of CRDs and the 7TM (C), the VFT and 7TM domains (D). The inter-protomer dynamics between the VFT, the B2' module, the second A1 module of CRDs, and the 7TM domains are quantified by measuring the distance distributions between LB2-LB2 COM, B2'-B2' COM, D560-D560 Cα and TM6-TM6 COM, respectively. Scatter points represent simulation snapshots taken at 20ns intervals.

(2) *It is not clear which of the intra-domain CRD conformations observed during the simulations (Figure 4) are found in which of the S1 to S5 states.*

We have incorporated detailed information on how the intra-domain CRD conformations (Figure 4) correspond to the S1 through S5 states (Figure S7). Since the intra-domain CRD conformation a_1 constituted the predominant group, it was unsurprising to find both protomers in the S1, S3, and S5 states exhibiting the a_1 conformation. Consistently, in the S2 state, both protomers displayed the a_2 intra-domain CRD conformation, characterized by a lateral rotation of the B2' modules. This rotation facilitated the formation of the B2' interface observed in the S3 state. Furthermore, in the S4 state, protomer A adopted the a_4 conformation, characterized by an extension of the first A1 module, which triggered the re-orientation of the 7TM interface.

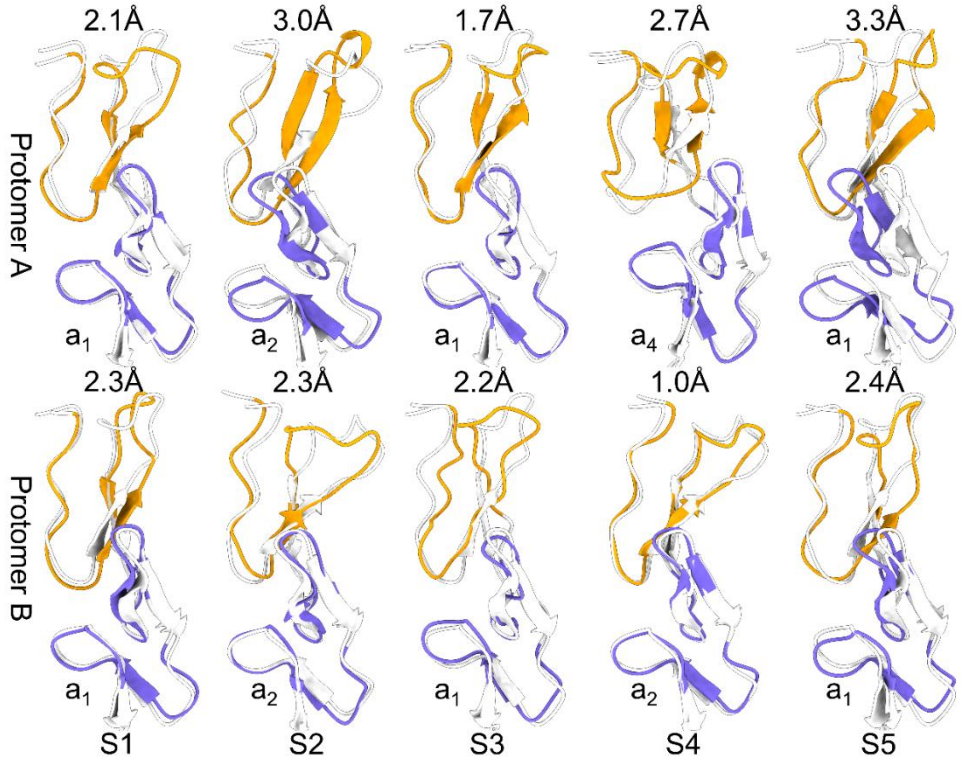

Figure S7. The intra-domain conformation of CRD across the metastable states. For each metastable state, protomers are aligned to the representative intra-domain CRD conformation that most closely matches, determined by the smallest Cα RSMD. The label for the corresponding representative intra-domain CRD conformation is positioned at the lower left of each structure, and the RMSD value is noted at the upper center.

(3) *However there seems to be a discrepancy in particular the S1 state in Figure S8 does not seem to correspond to the initial symmetrical resting conformation. This needs to be clarified.*

This discrepancy can be attributed to the moderate inter-domain dynamics of CRDs, even in the inactive state of mGlu5. Figure S8 showed the distance distribution between residue D560, the analogous position where donor and acceptor fluorophores were placed in the smFRET experiments (Liauw et al., *Nat Chem Biol*, **2021**, 17(3):291-297). This distribution showed that CRDs exhibited moderate inter-domain dynamics even in the inactive state of mGlu5, as evidenced by 97% of the conformations fluctuating between 68.0 Å and 78.0 Å. Consistently, in the apo inactive cryo-EM structure, the distance is 68.3 Å (PDB ID: 6N52). In the antagonist-bound inactive cryo-EM structure, the distance is 70.2 Å (PDB ID: 7FD9, Nasrallah et al., Cell Rep, 2021, 36(9):109648). In the CDPPB-bound inactive cryo-EM structure, the distance is 73.4 Å (PDB ID: 8T6J, Kumar et al., *bioRxiv*, **2023**, 2023.08.29.555158), which is close to the metastable state S1 (74.3 Å). This variability further highlights the inherent flexibility within the CRDs, even in the inactive states.

(4) *To support their results, the authors introduced some mutations from Arg524 to*

Trp532 and performed functional assays but they did not enumerate in what residues they were mutated into. This needs to be added and interpreted according to the mutations.

We mutate the residues from Arg524 to Trp532 into alanine to verify the functional importance of the B2' module. Our simulations revealed the role of the B2' module in mediating the active CRDs interface. In the revised manuscript, this active CRDs interface was confirmed by introducing a cysteine-mediated crosslink at the potential interface of the B2' module (I523C). As shown by the replotted Figure 4C and D, the I523C mutant maintained comparable levels of cell surface expression but demonstrated a robust constitutive activity as high as the glutamate-induced activity in the wild type (WT). Mutating the I523 residue to alanine (I523A) or altering its adjacent two residues (K521&V522&I523A, I523&R524&K525A) led to the absence of constitutive activity and a significant reduction in efficacy, yet cell surface expression levels remained similar to those of the WT. We have added these results in the revised main text.

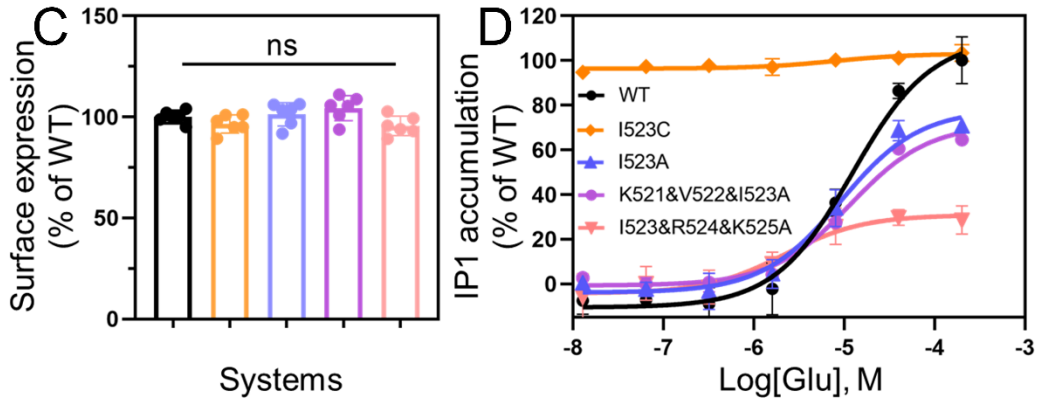

Figure 4. Experimental verification of the observed CRD association dynamics. (C) Quantification of cell surface expression. Data are presented as mean ± s.e.m. of six independent experiments. ns, not statistically significant (one-way ANOVA with Dunnett's post hoc test). (D) Crosslinking at the potential surface of the B2' module by an I523C mutant displays high constitutive activity, as measured using IP accumulation. Alanine mutation of critical residues involved in forming the observed B2'-mediated interface blunt glutamate-induced signaling compared to the WT. Data are presented as mean ± s.e.m. of three independent experiments.

4) When introducing the analysis of the 7TM domain dynamics of their work, the authors recall the TM6–TM6 interface reorientation and the G-protein binding cavity. a. The cited references are incomplete. They should cite and comment on the recent cryo-EM mGlu5 structures disclosed in a recent article from the Kobilka's group (Kumar et al BioRxiv 2023 and structures available at the Protein Data Bank). They should also better report on the stabilizing role of G-protein and positive allosteric modulators (e.g., Cao et al. Nature Com 2021, Lecat-Guillet et al. Sci Adv 2023, Cannone et al. BioRxiv2023) besides a comment on "dynamic allostery" and citing reference 43.

RESPONSE: Thank you for your insightful comments. Kumar et al. have recently released four cryo-EM structures of mGlu5. We will compare the structures with our proposed models one by one in your following *comment 4d*. To address your comments and extend our models of mGlu5 activation, we conducted additional extensive unbiased all-atom MD simulations on different full-length mGlu5 systems (Agonist + PAM and Agonist + PAM + G_q). We want to transfer to your following *comment 4c* to discuss our mechanistic insights into the full activation of mGlu5 upon G_q coupling.

Here, we report our new findings that PAM may enhance mGlu5 activation via conformational bias. Compared to the system where only agonists were added (1 μs × 10 independent MD simulations referencing PDB ID: 6N51), the PAM CDPPB-bound protomer exhibited an outward movement of TM6, decreasing the TM6-TM6 distance and likely leading to a more compact TM6-TM6 interface (Figure S14A). To quantify this, we calculated the interaction free energy between the 7TMs employing the molecular mechanics/generalized Born surface area (MM/GBSA) method. The inclusion of PAM CDPPB significantly strengthens the interaction at the 7TM dimer interface, with an interaction energy of -16.8 ± 7.3 kcal/mol compared to -2.5 ± 4.9 kcal/mol in the absence of PAM CDPPB (Figure S14B). This result validated a more stabilized active 7TM interface in the presence of PAM CDPPB (Cao et al., *Nat Commun*, **2021**, 12(1):5426; Lecat-Guillet et al., *Sci Adv*, **2023**, 9(22):eadf1378; Cannone et al., *bioRxiv*, **2023**, 2023.11.07.565819).

Utilizing Bimane fluorescence, Kumar et al. observed a notable conformational change in the ICL2 upon the addition of PAM CDPPB, distinguishing this effect from that observed with the agonist alone. Although the sensor revealed discrete conformations of ICL2 upon PAM binding, it did not resolve ICL2 structural compositions. Therefore, we generated the conformational landscape of ICL2 from the extensive simulation trajectories (1 μs × 10 repeats × 15 systems). It unveiled that ICL2 existed in a dynamic equilibrium, fluctuating between “closed” or “collapse” states that may occlude the intracellular cavity, and “open” or “extended” states that could facilitate receptor-effector interactions and promote receptor activation (Figure S14C and D). The presence of glutamates alone failed to significantly affect this equilibrium, suggesting that orthosteric agonists by themselves were insufficient to stabilize an active ICL2 conformation. In contrast, the addition of PAM CDPPB, or PAM CDPPB in combination with G_q to the glutamate-bound mGlu5, markedly shifted the equilibrium toward an active ICL2 state, characterized by an appropriately open and extended conformation. Consequently, we proposed that PAM binding transitioned ICL2 from the inactive closed or collapsed states which might impede the G_q protein binding, to the active open and extended states which can bind to the G_q protein.

These findings collectively demonstrated that PAM exerted its positive allosteric modulation effect on mGlu5 by stabilizing not only the active inter-domain 7TM interface but also an appropriately open and extended intra-domain ICL2 conformation. The detailed information has been updated as a supplementary information part (Supplementary Note 6).

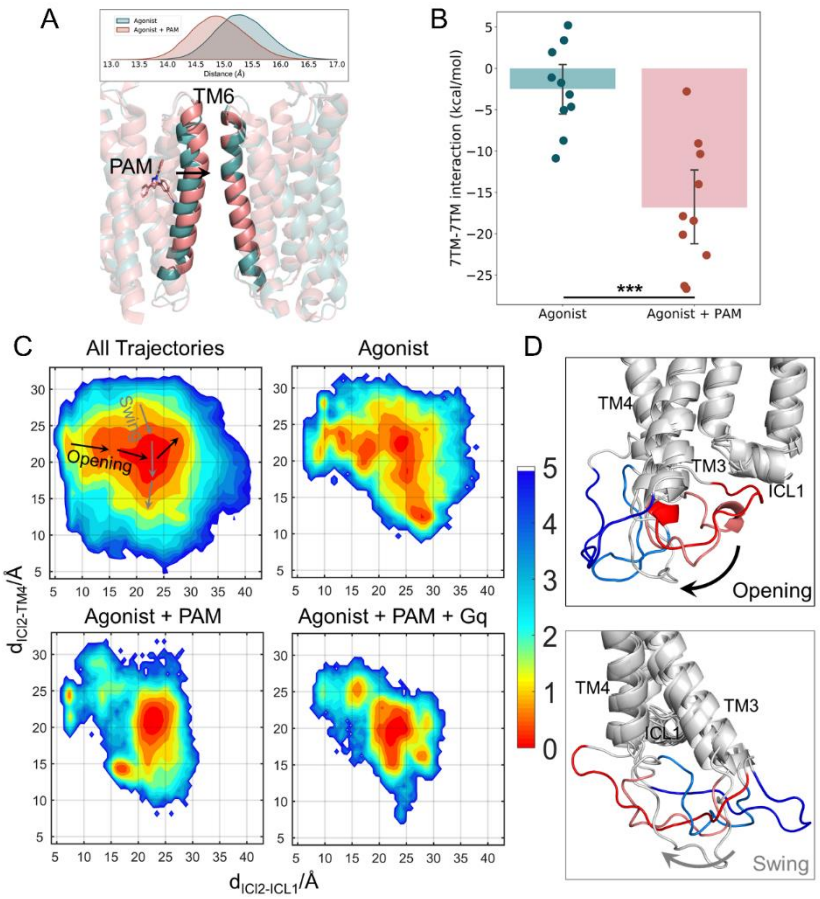

Figure S14. Conformational changes upon CDPPB binding to the mGlu5. (A) The CDPPB, glutamate-bound representative structure (red) exhibits notable proximity trends at the TM6-TM6 interface, as highlighted by the arrow, in comparison to the structure bound with glutamate alone (green). This observation is supported by the quantitative analysis of the distance distribution, specifically measured by the W785$^{6.50}$ Ca-Ca distance. (B) The interaction free energy of the 7TMs (kcal/mol) was calculated using the MM/GBSA method (Reference). The data are presented as mean ± s.e.m. derived from ten independent MD simulations based on the agonist-bound structure (PDB ID: 6N51) and the agonist, PAM-bound structure (PDB ID: 8TAO). Statistical analysis of the differences between these two systems was conducted using a two-way ANOVA, followed by Dunnett's post hoc test ($P < 0.0001$). (C) The conformational landscape of ICL2 derived from simulations. The *x*-axis ($d_{ICL2-ICL1}$) was defined as the distance between the Ca atom of C681 on the ICL2 and the center of mass (COM) of all Ca atoms of ICL1, reflecting the opening motion of ICL2 with increasing $d_{ICL2-ICL1}$ values. The *y*-axis ($d_{ICL2-TM4}$) was determined using the distance between the Ca atoms of C661 on the ICL2 and C691$^{4.30}$ on the TM4, the same points of the fluorescence experiments, representing the swinging motion of ICL2. (D) Representative structures of mGlu5, showcasing the varied conformations of ICL2.

b. When monitoring the conformational orientations of the TM6–TM6 interface, the authors identified three metastable states (M1, M2, and M3). They need to link these states to the S1 to S5 states defined previously in the manuscript. Is M4 in Figure 5C

corresponding to M3, it is not mentioned in the text? A transit intermediate between M1 and M2 is also cited. Altogether, data in this paragraph are not well presented. It needs to be improved.

RESPONSE: We appreciate your suggestions. Yes, the label M4 in Figure 5C actually corresponds to M3. As per your suggestions, considering the similar positions within each respective free-energy basin, we linked M1 to S3 and M3 to S5 (Figure R3).

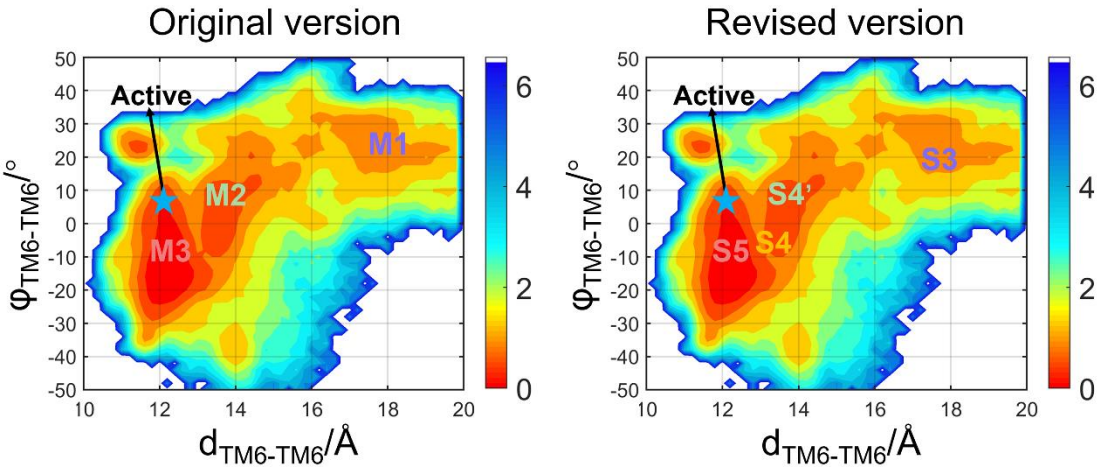

Figure R3. The revised conformational landscape of the TM6-TM6 reorientation.

Notably, the S4 state is located in the lower portion of its basin while M2 is in the upper portion, promoting us to associate M2 with an alternative S4' state. To enhance clarity and readability, we have restructured this paragraph as follows:

"Focusing on the region where the TM6-TM6 interface begins to form, the S3 to S5 states were located within three predominant free-energy basins (Figure R3). In S3, with $\varphi_{TM6\text{-}TM6}$ of 25.3°, the B2' modules of CRDs initiated mutual interactions, while the A1 modules remained separate (Figure S6). Transitioning to S4, the first A1 module of protomer A assumed the configuration depicted in Figure 4a$_4$, yielding a $\varphi_{TM6\text{-}TM6}$ of -8.7°. Given that the representative conformation of the S4 metastable state was situated in the lower portion of the basin, further analysis revealed an alternative conformation, S4', in the upper portion. In this state, the first A1 module of protomer B also adopted the Figure 4a$_4$ configuration, leading to an intermediate $\varphi_{TM6\text{-}TM6}$ of 9.8° (Figure 5C). These sequential conformational changes of CRDs in both S4' and S4 might be amplified through their crucial interactions with ECL2s, ultimately triggering a 20° rotation in the 7TM domain during activation. Furthermore, the free-energy basin where S5 is located suggests that the TM6-TM6 orientation seen in 6N51 likely denotes a pre-activation state, supported by the trend towards a -8.7° orientation in S5, and even extending to -20° (Figure R3). The negative orientations have been observed in recent experimental findings with G protein-stabilized fully active conformations of class C GPCRs ranging from -2.3° in the mGlu2-G$_i$ complex to -20.6° in the mGlu4-G$_i$ complex (Table S2)".

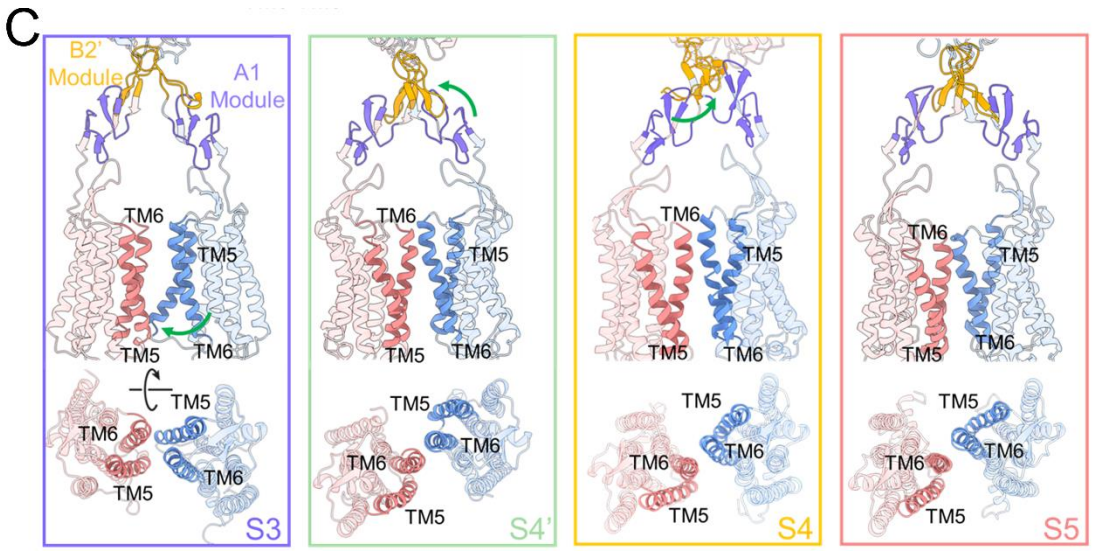

Figure 5C. Representative structures within the 7TM reorientation process. Each structure is presented in a box-colored corresponding to (Figure R3). The top half of the box provides a frontal view of mGlu5, while the bottom half provides a top view of the 7TM domain. TM5 and TM6 are highlighted to display their orientation. Significant movement patterns are indicated by green arrows.

c. It is now admitted that a fully active state of mGluRs can only be reached when a G-protein is bound to the receptor. Can the G-protein be added in the models? This would give a better insight into the activation mechanism from resting to fully active state. Moreover, the functional assays with the various mutants are run in HEK293T cells where the G-protein is present.

RESPONSE: We totally agree with your insight that a fully active state of the mGlu receptors can only be reached when the G protein is coupled. To the best of our knowledge, the structure of the G protein-coupled mGlu5 complex has not been discovered, leaving the full activation mechanisms of mGlu5 largely unexplored. In general, mGlu5 couples with G_q protein. To bridge this gap, we employed Alphafold2-multimer to generate the structure of mGlu5-G_q complexes.

To simplify the prediction process and highlight the significant interaction regions (mainly involving the α5 helix), we opted for the mini-G_q protein sequence due to its small size. The highest-ranked predicted structure seemed reasonable, evidenced by the high confidence scores of most residues and a similar G_q insertion mode compared to the recently released CASR-G_q cryo-EM structures. Next, we aimed to further enhance the reliability of the predictive mGlu5-G_q complex model by leveraging the just available high-quality crystal structures of the mGlu5 homodimer. The relative position of mGlu5 and downstream mini-G_q was preserved, and the object GPCR was aligned to the most representative active structure of the mGlu5 receptor (PDB ID: 8TAO), referred to all Cαs in the object GPCR. This alignment was refined over five cycles using the Executive RMS function in PyMOL. Following this, the fully active mGlu5 structure, bound with glutamate, PAM CDPPB, and mini-Gq, underwent further refinement by extensive minimization cycles until convergence was achieved.

Eventually, 10 independent classical MD simulations, each lasting 1.0 μs, were performed on this refined, fully active mGlu5 structure.

To explore detailed interaction variations at the mGlu5-7TM-G_q interface, we carried out tICA focusing on the interface contacts. An interface contact was defined as any pair of residues on the mGlu5-7TM and those on the G_q protein, with a closest distance threshold set at 5 Å. The resulting free energy landscape established by the first two tICs revealed three predominant interaction modes (< 0.5 kcal/mol, labeled G1, G2, G3). A notable conformational shift observed is the tilting of the α5 helix, which exhibited a maximum tilt of approximately 23.3° in G1 compared to its orientation in G3. Such conformational changes of the α5 helix are also captured in the formation of the fully active NTSR1-G_{i1} and β_2AR-G_s complexes (Kato et al., *Nature*, **2019**, 572(7767):80-85; Mafi et al., *Nat Chem*, **2023**, 15(8):1127-1137).

Consistently, the G3 state appeared to be a pre-coupled G_q binding mode, exhibiting minimal insertion into the cavity. This state retained the two key inactivation-stabilizing 'ionic-lock' motifs: a salt bridge between $K665^{3.50}$ and $E770^{6.35}$, and a hydrogen bond between $R668^{3.53}$ and $S614^{2.35}$. Accordingly, the binding energy for G3, as determined through the MM/GBSA method, is the least favorable, approximately -46.8±13.2 kcal/mol. In contrast, the G1 state likely represented a fully activated conformation, wherein the ionic-lock motifs were completely disrupted. Moreover, the active-state asymmetric TM6-TM6 interface was formed, with an upward shift in TM6 of the G_q-coupled protomer facilitating the rearrangement of ICL3. This conformational rearrangement orchestrated the cytoplasmic tip of TM3, ICL2 and H8 (potentially the C terminus) to envelop the α5 helix of G_q. Owing to these comprehensive interactions, the G1 binding mode was the most energetically favorable (-86.3±17.4 kcal/mol). In addition, the α5 helix formed moderate interaction networks with the 7TM domain in G2, resulting in a binding energy of -68.9±15.7 kcal/mol. Therefore, G2 may represent an intermediate state along the full activation pathway for mGlu5-G_q.

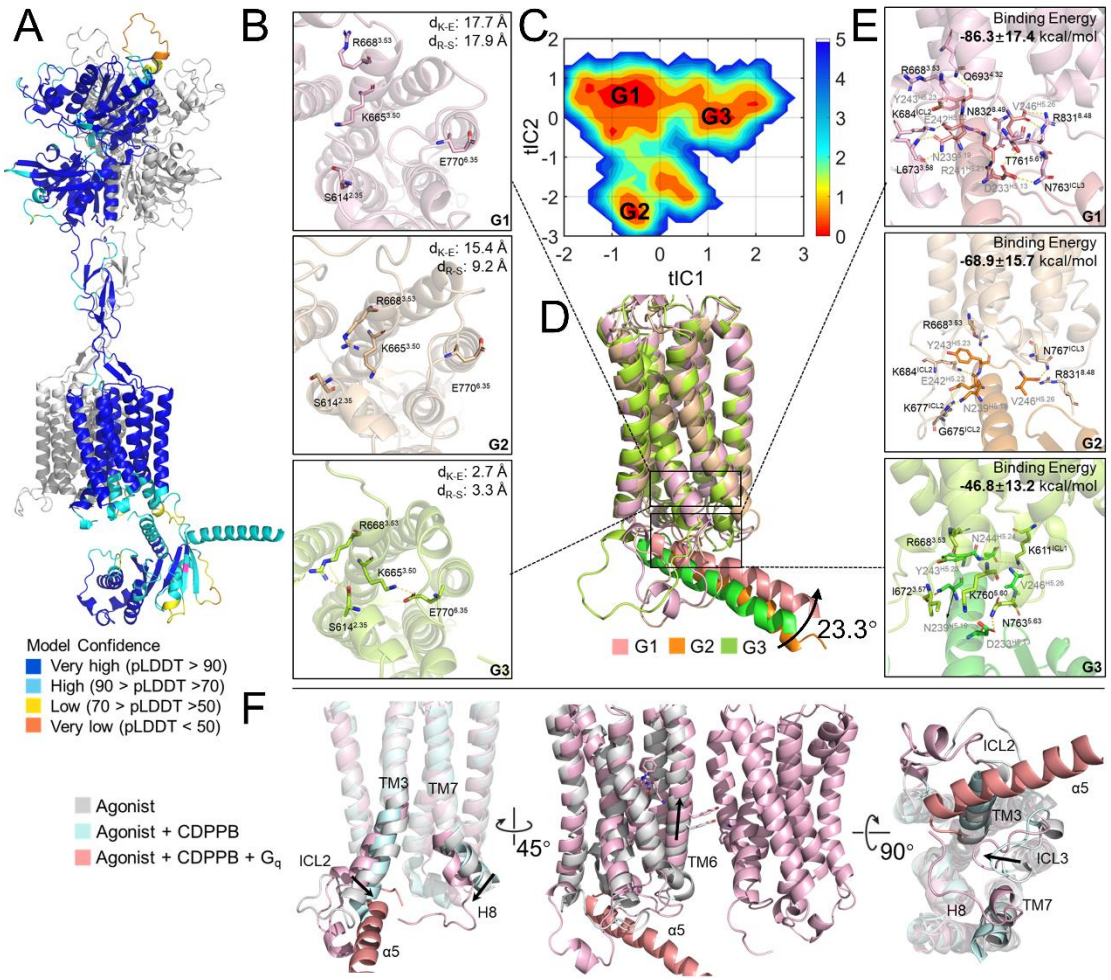

Figure S15. Dynamics of the G_q coupling to mGlu5. (A) Predicted mGlu5-G_q complex structure, color-coded by the predicted local distance difference test (pLDDT) score for evaluating model confidence. (B) Illustration of 'ionic-lock' motifs in metastable states during G_q coupling. The distance between $K665^{3.50}$ and $E770^{6.35}$ ($d_{K\text{-}E}$) is measured from the Nz atom of K and the closest Oe atom of E. The distance between $R668^{3.53}$ and $S614^{2.35}$ ($d_{R\text{-}S}$) is measured from the Og atom of S to the nearest Nh atom of R. Polar interactions are represented with yellow dashed lines. (C) Free energy landscape derived from the first two tICs, with each local free energy minimum labeled by its corresponding metastable state. (D) Representative mGlu5-G_q structures, showcasing the variety of G_q binding modes. (E) The detailed interaction networks between mGlu5 and G_q, with binding free energies calculated via the MM/GBSA method and summarized in the upper right corner. (F) Comparison of the 7TM bundle from the CDPPB-bound protomer (PDB ID: 8TAO) and the agonist-bound protomer (PDB ID: 6N51) to that of the G_q-coupled protomer of G1. TM6 of the G_q-coupled protomer is noted for its tilt and shift of nearly half a helical pitch towards the extracellular side, resulting in an asymmetric TM6-TM6 interface. Arrows highlight the consequential conformational arrangement, particularly in the cytoplasmic end of TM3, intracellular loops (ICL2 and ICL3), and the H8 helix.

d. The reported results should be compared to the recent cryo-EM structures and the sequential mGlu5 activation pathway recently disclosed. The authors should put forward what new information they provide with a molecular modeling approach in comparison to the structural and biophysical approaches.

RESPONSE: Kumar et al. have released four cryo-EM structures of mGlu5, including Quis-bound intermediate 1a (PDB ID: 8T7H), Quis-bound intermediate 2a (PDB ID: 8T8M), Quis and CDPPB-bound intermediate 3a (PDB ID: 8TAO), and CDPPB-bound inactive intermediate 1b (PDB ID: 8T6J). Firstly, let us compare the structures identified recently with our proposed models individually. Subsequently, we will summarize the strengths and the novel insights offered by MD simulations in contrast to structural and biophysical methods.

(1) **Quis-bound Intermediate 1a:** The Intermediate 1a exhibits an Rcc conformation, characterized by two closed VFTs domains while the CRDs and 7TMs remain as far apart as in the inactive mGlu5 state. In alignment with this, our in-depth analysis of the S2 metastable state identified an alternative configuration of the VFTs (denoted as S2', minimal Cα RMSD to Intermediate 1a: 3.8 Å), in which the VFT of protomer A transitioned from an open (S2, Rco) to a nearly closed state ($RMSD_{VFT}^{A}$ = 1.8 Å), closely approaching an Rcc conformation (Figure 3B). Moreover, Cannone et al. have captured a transient and non-classic binding pose of quisqualate (a glutamate analogue) in the Rcc conformation of mGlu5. Similarly, our simulations also captured the dynamic binding poses of glutamate, particularly within the S2 state (Figure S4), highlighting the substantial flexibility of the VFT domains. We have added the comparison in the revised manuscript accordingly throughout the text and figures (Figure 3 and Supplementary Note 4)

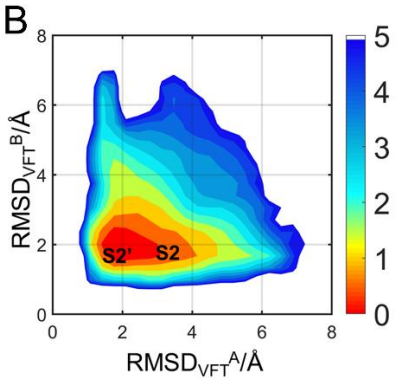

Figure 3B. A per-protomer analysis of the S2 metastable state uncovered an alternative configuration of the VFTs, termed S2'.

(2) **Quis-bound Intermediate 2a:** The Intermediate 2a, simultaneously stabilized by Quis and Nb43 exhibits a conformation remarkably similar (Cα RMSD = 2.3 Å) to the structure of 6N51 (also complexed with Quis and Nb43) determined by the Kobilka lab in 2019. Both structures are identified within the S5 through our simulations (minimal Cα RMSD = 2.2 Å).

Significantly, our simulations uncovered two additional metastable states, S3 and S4, which might bridge the Intermediate 1a and 2a. These transient metastable

states may prove challenging to stabilize by cryo-EM. In these metastable states, we revealed the role of the B2' module in mediating the active CRD interface (see our responses to your comment *3.4*).

(3) **Quis and CDPPB-bound Intermediate 3a:** Kumar et al. observed an asymmetric TM6-TM6 interface in Intermediate 3a, highlighting the critical asymmetric microswitch $Y799^{6.44}$. These asymmetric features, although absent in earlier apo (PDB ID: 6N52) and active (PDB ID: 6N51) mGlu5 structures that are endpoints of our simulations, have been successfully captured in our extensive simulations and the critical role of $Y799^{6.44}$ in receptor activation has been confirmed through our site-directed mutagenesis experiments (Figure 5).

In addition, Kumar et al. failed to determine the ICL2 conformation in the cryo-EM structure of Intermediate 3a. Utilizing Bimane fluorescence, they observed a notable conformational change in the ICL2 upon the addition of CDPPB, distinguishing this effect from that observed with the agonist alone. Although the sensor revealed discrete conformations of ICL2 upon PAM binding, it did not resolve ICL2 structural compositions (see our responses to your comment *4a*).

(4) **CDPPB-bound inactive Intermediate 1b:** Although Intermediate 1b is beyond the scope of our research, it inadvertently validated the moderate inter-domain dynamics within the CRDs, even when mGlu5 is inactive, as demonstrated in our simulations (see our responses to your comment *3.2*)

(5) **The novel insights from MD simulations:** As shown in Figure 7, the $^{\#}$ superscript represents a conformational state confirmed through both cryo-EM experiments and MD simulations, as we discussed earlier. The other dynamic intermediates encapsulate the novel insights we have gleaned from our study, which are beyond the static cryo-EM or indirect smFRET experiments. We have reorganized the discussion paragraph and believe that this revision may answer your concerns.

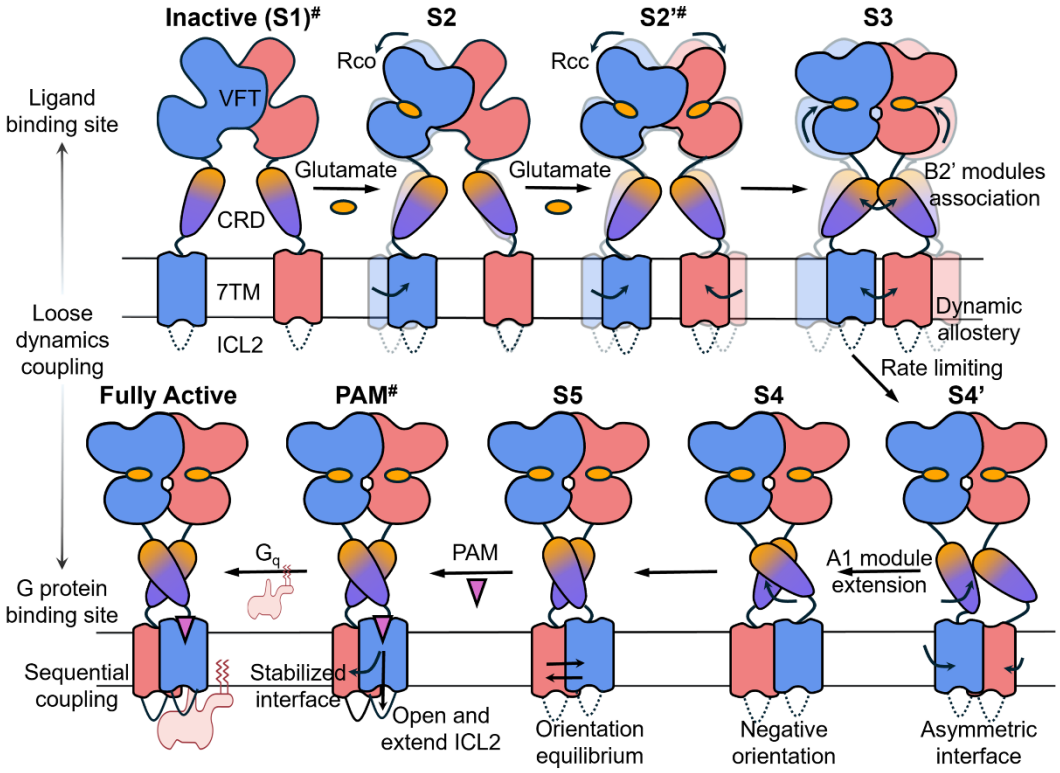

Figure 7. Schematic of the asymmetric stepwise activation model for mGlu5.

Long timescale simulation of mGlu5 unveiled novel, detailed atomic-level insights into the activation mechanisms of dimeric class C GPCRs (Figure 7). Initially, upon agonist loading, we observed the co-existence of transient Rco (S2) and Rcc (S2') conformations, accompanied by a sequential closing of VFTs. Unlike previously established classic binding modes in the active state, glutamate exhibited dynamic binding positions in these intermediate states, indicating substantial flexibility within the VFT domains. During the peer-review process, a transient Rcc state with the non-classic binding pose of quisqualate (a glutamate analogue) was identified through cryo-EM experiments, lending experimental support to our computational model. Subsequently, the activation signals from VFTs seemed to be amplified by the crucial apical modules (B2' modules) of the CRDs. The B2' module not only engages laterally with the neighboring B2' module—amplifying the signal for the TM6–TM6 interface formation (S3)—but also interacts with the extended A1 module of the adjacent protomer, further modifying the TM6–TM6 interface orientation (S4' and S4). The simulations underscore the highly flexible nature of CRDs, a trait potentially common across all mGlu receptors (Reference). This flexibility enables the precise association of CRDs, which is sufficient for full mGlu activation, confirmed by a robust constitutive activity after the introduction of a cysteine-mediated crosslink at the potential surface of the B2' module (I523C).

Meanwhile, from S3 to S4, dynamic allostery played an underemphasized role in conjunction with dimerization. As the "active" TM6-TM6 interface formed asymmetrically and underwent negative reorientation, the flexibility of the 7TM significantly increased, facilitating the reorganization of conserved motifs and

residue networks within the 7TM domain. Dynamic allostery has also been identified as a regulatory mechanism in class B GPCRs, suggesting that it may be a ubiquitous regulatory mechanism in GPCR signaling[43]. However, this active TM6-TM6 interface appeared not to be sufficiently stabilized by the orthosteric agonist alone, as indicated by its orientation equilibrium in S5. On the contrary, the addition of a PAM stabilized the inter-domain active TM6-TM6 interface, shifting the intra-domain ICL2 conformation from inactive closed or collapsed states, which impeded G_q protein binding, to an active open and extended state. Indeed, the involvement of ICL2 was validated by our pioneering effort to illustrate the dynamic interaction variations at the mGlu5-7TM-G_q interface. Besides the conformational arrangement of ICL2, in the unique fully active state (Fully active), the cytoplasmic tip of TM3, ICL3 and the H8 (potentially the C terminus) were also engaged to facilitate the G protein binding. Unlike family A and B GPCRs, which displace the cytosolic part of the TM6 helix to accommodate the G protein, family C GPCRs potentially utilize an alternative strategy by forming a pseudo-cavity between TM3, ICL2, ICL3 and receptor's terminus to coordinate the G protein.

Most importantly, it is extremely hard to disclose the conformation transition of a flexible multi-domain dimer in millisecond timescale by only classic MD simulations. In this study, we utilized a graded computational strategy progressing from two distinct structural endpoints through a minimum energy transition pathway (NEB without predefined collective variables) to an extensive free energy landscape (large-scale distributed MD simulations-based MSM). This strategy enabled us to reconstruct the millisecond-scale dimerization and long-range allosteric activation of mGlu5 at the atomic level. It significantly enhances the efficiency of simulation time compared to traditional brute-force simulations spanning several milliseconds. Most importantly, the adaptability of this strategy, especially without a curated definition of collective variables, suggests its potential applicability in characterizing millisecond-long events in other allosteric systems.

5) The correlation map to analyze movements between domains in the course of a biological pathway is a very powerful tool. Indeed Figure 6 provides a long-range connection between the VFT and the 7TM domains and between the adjacent protomers in the dynamics. Yet, since the binding of glutamate may not be correct in S1 and S2, the analysis may not be relevant.

Figure 6B does not give additional information compared to panel A.

RESPONSE: As we responded to your comment 2, the glutamate binding poses identified in S1 and S2 were obtained directly from unbiased MD simulations, aligning with results from prior simulation studies and recent cryo-EM structures.

Panel A in Figure 6 presents the Pearson correlation map, which describes the linear correlations. Since the inter-domain motions frequently exhibit nonlinear correlations, we employed mutual information analysis (Lange et al., *Proteins*, **2006**, 62(4):1053-1061). Indeed, this approach revealed additional significant long-range allosteric coupling between the 7TM domain and the VFT, CRD, and 7TM domains of the adjacent protomer.

6) In the discussion, putting forward that class C GPCRs dimerization may be useful for all GPCRs is not true because the mechanisms are quite different.
According to recent literature, active and fully active conformations of mGlu receptors should be distinguished.
In the first part of the manuscript, 5 states S1 to S5 are found and analyzed. Then in the discussion, the results are summarized in Figure 7 with only 4 states. This should be explained. This cartoon is very similar to that of Liauw et al. Nature Chem Biol 2021 (Figure 7). This similarity should be commented.

RESPONSE: Thanks for your questions, let us address each one in turn:

(1) In the discussion, putting forward that class C GPCRs dimerization may be useful for all GPCRs is not true because the mechanisms are quite different.

We agree with your comment and clarify that our discussion here is specifically limited to class C GPCRs:

"A comprehensive understanding of the dimerization and allosteric activation landscape is essential for the rational design of drugs aimed at modulating class C GPCR signaling in desired ways."

(2) According to recent literature, active and fully active conformations of mGlu receptors should be distinguished.

We agree with your suggestion and have defined only mGlu receptors stabilized by downstream G protein or mini-G protein as the fully active conformation.

(3) In the first part of the manuscript, 5 states S1 to S5 are found and analyzed. Then in the discussion, the results are summarized in Figure 7 with only 4 states. This should be explained. This cartoon is very similar to that of Liauw et al. Nature Chem Biol 2021 (Figure 7). This similarity should be commented.

We have updated Figure 7 to include all the metastable states identified in our study. The schematic model of the mGlu receptors is widely used (Koehl et al., *Nature*, **2019**, 566(7742):79-84; Kumar et al., bioRxiv, 2023, 2023.08.29.555158), and our proposed models offer a much more comprehensive depiction.

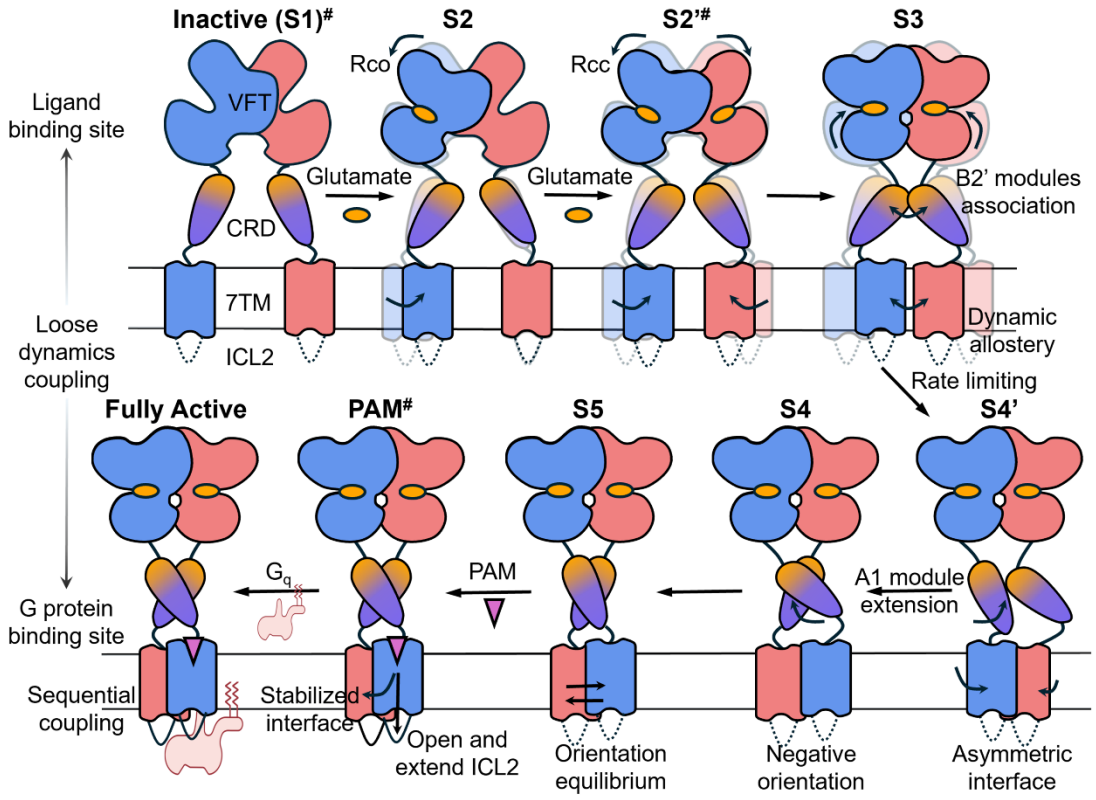

Figure 7. Schematic of the asymmetric stepwise activation model for mGlu5. The stepwise model for the allosteric activation mechanism of mGlu5, illustrating the conformational transitions from the inactive apo state through six intermediate states bound by agonist, to the agonist- and PAM-bound active state, and finally to the Gq-coupled fully active state, with a full-length view in schematic representation. Initially, in the absence of an orthosteric agonist (e.g., glutamate), mGlu5 resides in the apo inactive state (S1). The introduction of orthosteric agonist initiates its sequential binding (S2 and S2'), loosely triggering the conformational rearrangements within the 7TM domains. The closure of both VFTs further brings the protomers into proximity, leading to the initial association of CRDs through the B2' module. Next, the two A1 modules extend outward (S4' and S4), their action magnified by crucial interactions with ECL2, forming an asymmetric and negatively oriented "active" TM6-TM6 interface. This active interface may not be sufficiently stabilized by the orthosteric agonist alone, leading to a reversion to the equilibrium orientation of the TM6-TM6 interface (S5). In contrast, the addition of a PAM stabilizes the active TM6-TM6 interface, modulating the ICL2 conformation to an open and extended state (from dash to solid representation). Further coupling of a G_q protein results in a unique fully active conformation (Fully active), facilitating the transduction of intracellular signals. The $^{\#}$ superscript represents a conformational state confirmed through both cryo-EM experiments and MD simulations.

Specific comments

1) In Cao et al. (Nature Com 2021) and Kumar et al. (BioRxiv2023), the crucial type of membrane lipids used in assays is exposed. The authors used the classical POPC to

simulate the bilayer membrane. They should check the impact of this choice on the kinetics.

RESPONSE: Thanks for your questions. Cao et al. evaluated and obtained the optimized detergents for mGlu2-solubilization. However, Kumar et al. showed that in detergent micelles, there was no activation of G_q by mGlu5 bound to L-quisqualic acid, in contrast to a POPC/POPG lipid mixture membrane.

The types of lipids may have an impact on the kinetics. Nevertheless, our manuscript primarily focuses on elucidating the dynamic pathway of mGlu5 activation. In response to Comment *1*, the similar kinetics calculated from our simulation to the experiments (Grushevskyi et al., *Proc Natl Acad Sci U S A*, **2019**, 116(20):10150-10155) was used to reinforce the credibility of our MSM with biological observations, complementing the model's mathematical validation through the rigorous implied timescale test and the Chapman-Kolmogorov test. In addition, pure POPC membrane is a widely-used GPCR environment during MD simulations, which have provided considerable important conformational changes of the class A, B and C GPCRs (Dror et al., *Proc Natl Acad Sci U S A*, **2011**, 108(46):18684-18689; Kohlhoff et al., *Nat Chem*, **2015**, 2014;6(1):15-21; Suomivuori et al., *Science*, **2020**, 367(6480):881-887; El Daibani et al., *Nat Commun*, **2023**, 14(1):1338; Mattedi et al., *Proc Natl Acad Sci U S A*, **2020**, 117(27):15414-15422; Thibado et al., *Elife*, **2021**, 10:e67027). Thus, we followed these protocols and built a pure POPC membrane in the simulations. In the revised methods section, we have also referenced other MD researchers who utilized a pure POPC membrane, noting that this choice may have an impact on the kinetics.

2) In all figures where a free energy profile is displayed, the color scale should be mentioned in the legend. Same remark for the scale in Figure S9

RESPONSE: Thanks for your kind reminder. The color scales of all the free energy profiles and Figure S9 have been added to the legend.

Simulations should be able to describe the film and kinetics of the pathway between 3D-structures provided by structural biology. But the multiple virtual steps need to be validated. In the work of Li et al, an interesting approach is used but some results are questionable.

Altogether this manuscript lacks clarity and rigor. The authors need to show better what critical information they provide in comparison to that from literature.

RESPONSE: Thank you for the constructive critiques you have provided. We have tried our best to verify the multiple virtual steps in our simulations by providing further explanations and supplying experiments, which substantially improve the quality of our work. Thereafter, let us address the critical information beyond the literature as follows:

Firstly, our graded computational strategy is novel and generalizable. This strategy enhances the efficiency of simulation time compared to traditional brute-force simulations spanning several milliseconds. Therefore, it enabled us to reconstruct the millisecond-scale dimerization and long-range allosteric activation of mGlu5 at the atomic level. Most importantly, the adaptability of this strategy, especially without a curated definition of collective variables, suggests its potential applicability in

characterizing millisecond-long events in other allosteric systems.

Secondly, the long timescale simulation of mGlu5 unveiled novel, detailed atomic-level insights into the activation mechanisms. **1)** We observed the co-existence of transient Rco (S2) and Rcc (S2') conformations. Unlike previously established classic binding modes in the active state, glutamate exhibited dynamic binding positions in these intermediate states, indicating substantial flexibility within the VFT domains. **2)** We reveal the critical role of the B2' module of the CRD in the dimerization of mGlu5. The B2' module not only engages laterally with the neighboring B2' module—amplifying the signal for the TM6–TM6 interface formation (S3) —but also interacts with the extended A1 module of the adjacent protomer, further modifying the TM6–TM6 interface orientation (S4' and S4). **3)** We demonstrate that dynamic allostery plays an underappreciated role in mGlu5 activation, facilitating the reorganization of conserved motifs and residue networks within the 7TM domain (S3, S4', S4, S5). **4)** We unveil that PAM exerts its positive allosteric modulation effect by stabilizing not only an active tight inter-domain 7TM interface but also an appropriately open and extended intra-domain ICL2 conformation. **5)** We provide mechanistic insights into the full activation of mGlu5 upon G_q coupling for the first time, including the detailed interaction variations at the mGlu5-7TM-G_q interface in addition to the ICL2.

Reviewers' comments:

Reviewer #1 (Remarks to the Author):

The revised version of the manuscript presents considerable improvement with additional simulation and experimental data. It contains several novel findings that could impact future research, including: 1) A practical graded computational strategy for characterizing millisecond-long events in other allosteric systems. 2) A comprehensive dynamic pathway for a dimeric GPCR, which goes beyond the insights provided by recent structural and biophysical approaches.

Therefore, I fully support the publication of this interesting paper.

Reviewer #2 (Remarks to the Author):

The authors have responded to the points from my first review adequately

Reviewer #3 (Remarks to the Author):

The authors have provided more technical details in the revised manuscript. It is now evident that this study suffers from significantly inadequate MD sampling. The results are incoherent with the rich experimental data on mGluRs in the literature. Despite the extensive computational efforts, the main question (step-wise activation mechanism) is poorly addressed.

The main technical issues are the follows:

1. The NEB model oversimplified this complex system.

Two distances (in VFT and TM6) were used to describe the multi-step multi-domain activation process. FRET studies have shown that for mGluR5 and other mGluRs, multiple conformations exist for each of the 3 domains of mGluRs, which are loosely coupled. Thus, it is critical to choose an appropriate set of collective coordinates/variables to describe the high-dimensional motions of mGluR dimers, e.g. intra-/inter-domain, intra-/inter-protomer distances/orientations or other relevant descriptors of activation.

Although the NEB calculations appear to have converged on the 2-distance space, it describes poorly the high-dimension problem.

The authors cited applications of NEB on various other proteins. However, these do not translate to a straightforward application on mGluRs. Notably, the authors consider the SARS-CoV-2 spike glycoprotein ectodomain to be "much more flexible and complex". This is not true: the cryo-EM

structures of this protein in open and close states show a much lower degree of conformational differences than the inactive and active states of mGluRs.

The oversimplified NEB model is the main cause of inadequate MD sampling of the conformational space that was based on the NEB images.

2. Lack of feature selection for tICA to construct the MSM model.

It is critical and non-trivial to identify the features that describe the slow dynamics of a system. Poorly selected features result in poor MSM models. There is no test or justification of feature selection in this manuscript. I have previously recommended a commonly used feature selection procedure, by calculating the VAMP-2 scores of various features in a cross-validated manner. Machine learning methods have also been developed in recent years (e.g. Mardt et al. Nat Commun 2018), which may ease feature selection.

The authors stated that the 2 tICs used were sufficient, while "more than 5 tICs and 500 microstates could lead to overfitting". The read underlying issue is that the feature used here (aligned Calpha coordinates) could not well capture the essential dynamics of this particularly complex system (even though Calpha coordinates have been used for MSM model building in some simpler cases).

3. Inconsistency with literature data.

The MSM model has been reconstructed using 10 ns lag time and concluded that mGluR5 dimer rearrangements during activation took place in 0.99 ms (3.54 ms in the initial manuscript). The authors stated that this agrees with the study by Grushevskyi et al. PNAS 2019 on mGluR1. However, Grushevskyi et al. concluded that 1-2 ms corresponded to the initial rearrangements, followed by significantly slower changes in the TM domain (~ 20 ms). This aligns with other studies on mGluR1 that the VFT activation occurs rapidly in few ms, while the full activation takes place in dozens of ms (e.g. Hlavackova et al. Sci Signal 2012, Marcaggi et al. PNAS 2009).

The comparison with the latest data on mGluR5 by the Kobilka lab (Kumar 2023 bioRxiv) also shows discrepancies. For instance, the CRD-CRD distances here appear to describe 2-3 states, whereas 4 states have been shown by Kumar et al., similar to mGluR2 (Liauw 2021 Nat Chem Biol).

Fig.S3 also indicates that the 3 domains in the MD sampling have strong correlations (seemingly so from the histograms, while the correlations are not examined), rather than loosely coupled .

I hope these comments will help the authors improve the otherwise interesting study. The manuscript has merits but I do not recommend publication in its current form.

Reviewer #3 (Remarks to the Author):

The authors have provided more technical details in the revised manuscript. It is now evident that this study suffers from significantly inadequate MD sampling. The results are incoherent with the rich experimental data on mGluRs in the literature. Despite the extensive computational efforts, the main question (stepwise activation mechanism) is poorly addressed.

We sincerely thank the referee for their enthusiasm and constructive suggestions. Below, we have summarized our responses:

1. The NEB is not oversimplified, as it maps the transition pathway within the full Cartesian space without the need to define collective variables. The 2-distance collective variables are only for visualizing the major motions on a 2D figure.
2. The selection of features has been thoroughly justified by VAMP2 score in a cross-validated manner with a variety of distance features.
3. Our revised manuscript reveals a dual aspect of the stepwise activation mechanism: 1) Stepwise activation between subunits (inter-subunit arrangement), induced by successive agonist binding, was initially uncovered through NEB calculations and subsequent MD samplings in our original manuscripts. 2) Stepwise activation involves inter- and intra-subunit rearrangements, with the latter being triggered by G protein coupling. The intra-subunit rearrangements have been investigated via AlphaFold2-multimer predictions and subsequent MD samplings in our last revision, which could address the noted inconsistence with experimental data.

The main technical issues are the follows:

1. The NEB model oversimplified this complex system.

Two distances (in VFT and TM6) were used to describe the multi-step multi-domain activation process. FRET studies have shown that for mGluR5 and other mGluRs, multiple conformations exist for each of the 3 domains of mGluRs, which are loosely coupled. Thus, it is critical to choose an appropriate set of collective coordinates/variables to describe the high-dimensional motions of mGluR dimers, e.g. intra-/inter-domain, intra-/inter-protomer distances/orientations or other relevant descriptors of activation.

Although the NEB calculations appear to have converged on the 2-distance space, it describes poorly the high-dimension problem.

The authors cited applications of NEB on various other proteins. However, these do not translate to a straightforward application on mGluRs. Notably, the authors consider the SARS-CoV-2 spike glycoprotein ectodomain to be "much more flexible and complex". This is not true: the cryo-EM structures of this protein in open and close states show a much lower degree of conformational differences than the inactive and active states of mGluRs.

The oversimplified NEB model is the main cause of inadequate MD sampling of the conformational space that was based on the NEB images.

It's important to clarify that the NEB algorithm does not require the definition of collective variables; instead, it maps the transition pathway within the full Cartesian space. The NEB "springs" were applied to all protein atoms. We have highlighted this information in the Materials and Methods section; for additional metamaterial details, please refer to the section as well. The primary goal of the NEB calculations is to elucidate the inter-subunit rearrangement (protomer approximation) of mGluR5. The major inter-subunit rearrangement involves the compaction between the VFT and 7TM domains (see Figure 2C and E). To visualize these major movements on a two-dimensional figure, we employed the two distances (in VFT and 7TM) here, demonstrating the convergence of the NEB model for elucidating the inter-subunit rearrangement with more than 24 images. Therefore, the NEB model is not oversimplified.

The cited applications of NEB on various proteins are to show the validity of the algorithm and the typical selection of image numbers in biomolecular simulations. In terms of the SARS-CoV-2 spike glycoprotein ectodomain, we intended to highlight its flexibility and complexity in comparison to other proteins, not directly with mGluRs. To prevent any confusion, we have removed this description.

Furthermore, the convergence of the free energy landscape and transition pathway was validated by projecting the varied subsets of the MD conformations (aggregated time of 26μs, 52μs, 78μs, 104μs, 130μs) onto the two slowest tICs (see below Figure R1). It is clear that the free energy landscape reaches reasonable convergence, notably without the emergence of new metastable regions in the phase space as conformational sampling increased.

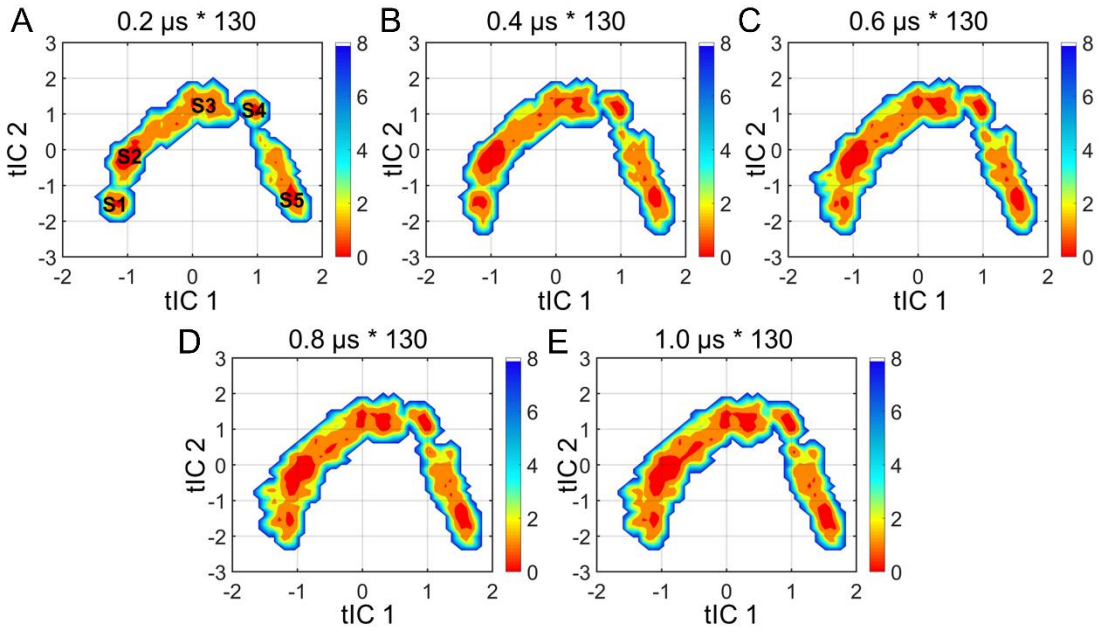

Figure R1. Convergence of the free energy landscape and transition pathway was validated by projecting the varied subsets of the MD conformations (aggregated time of 26μs, 52μs, 78μs, 104μs, 130μs) onto the two slowest tICs (unit in kcal/mol).

2. Lack of feature selection for tICA to construct the MSM model.

It is critical and non-trivial to identify the features that describe the slow dynamics of a system. Poorly selected features result in poor MSM models. There is no test or justification of feature selection in this manuscript. I have previously recommended a commonly used feature selection procedure, by calculating the VAMP-2 scores of various features in a cross-validated manner. Machine learning methods have also been developed in recent years (e.g. Mardt et al. Nat Commun 2018), which may ease feature selection.

The authors stated that the 2 tICs used were sufficient, while "more than 5 tICs and 500 microstates could lead to overfitting". The read underlying issue is that the feature used here (aligned Calpha coordinates) could not well capture the essential dynamics of this particularly complex system (even though Calpha coordinates have been used for MSM model building in some simpler cases).

We thank the reviewer for this good suggestion. To justify feature selection, we incorporated not only the aligned Cartesian coordinates but also various distance features.

For the distance features, to capture the slowest dynamics associated with the inter-

subunit rearrangement (protomer approximation) of mGluR5, various sets of distances were included. These were achieved by varying the heavy atom pairs between protomers in the active cryo-EM structure within a range of cutoffs. To incorporate as many distances as possible, nine cutoffs were considered, ranging from 7 to 15 Å, which yielded distance pairs ranging from 1,274 to 119,359. Finally, the closest heavy-atom distances between each pair of residues were calculated, denoted as $f(d) = \min(d)$, and we also applied an inverse transformation ($f(d) = d^{-1}$). Following Westerlund et al. (*PLoS Comput Biol*, **2022**, 18(10):e1010583), the different feature types were evaluated by using the VAMP2 score across five lag times (2 ns, 5 ns, 10 ns, 15 ns, 20 ns) using the top ten eigenvalues and five-fold cross-validation.

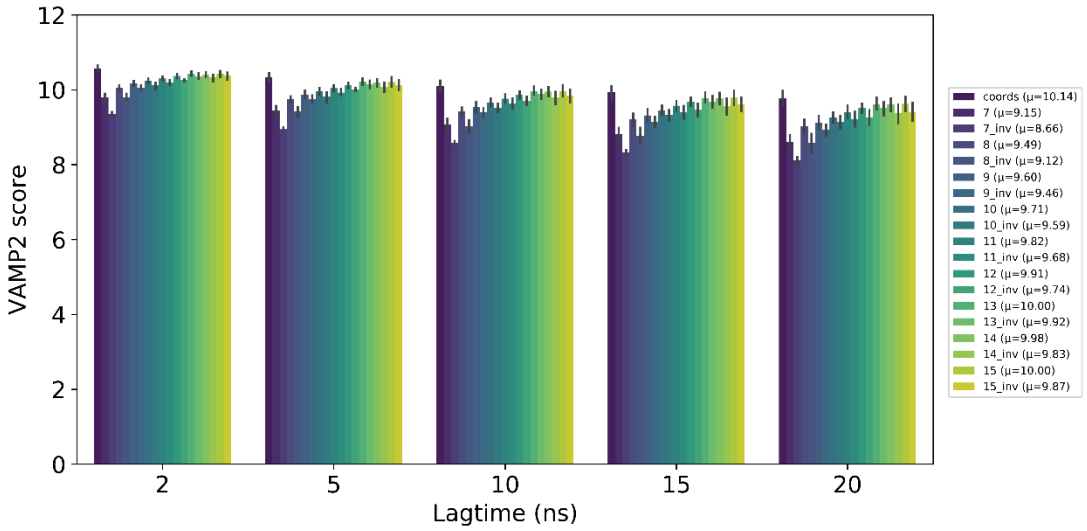

Figure R2. The feature selection by calculating VAMP2 scores of the 10 slowest processes for a variety of features at varying lag times. The mean VAMP2 scores from 5-fold cross-validation are plotted as bar and standard deviations are plotted as error bars.

The mean scores suggetsed that these feature types yield MSMs of comparable quality (Figure R2). For distance features, the choice of distances of a 13 Å cutoff (totaling 58,848) proved effective, as the introduction of additional atom pairs beyond this cutoff did not have substantial improvement. It suggests that the atom pairs within this range could sufficiently describe the slowest conformational dynamics. However, the aligned Cartesian coordinates achieved the highest mean VAMP2 score, thereby justifying this feature type as the most suitable for MSM construction.

The aligned Cartesian coordinates, which reflects the main chain movements of the protomer, is not only intuitively appropriate for capturing the essential dynamics of

inter-subunit rearrangement driven by the main chain's approach, but it is also statistically validated by the VAMP2 score. Furthermore, the power behind tICA is to disregard degrees of freedom that quickly decorrelate and merely contribute statistical noise. However, as the number of tICs increases, more noise is introduced, particularly for this flexible and complex mGluR5. A large number of tICs and microstates lead to overfitting: when the number of microstates is large, the MSM likely fits the statistical noise in the dataset rather than the underlying slow dynamical processes (McGibbon et al., *J Chem Phys*, **2015**, 142(12):124105).

3. Inconsistency with literature data.

The MSM model has been reconstructed using 10 ns lag time and concluded that mGluR5 dimer rearrangements during activation took place in 0.99 ms (3.54 ms in the initial manuscript). The authors stated that this agrees with the study by Grushevskyi et al. PNAS 2019 on mGluR1. However, Grushevskyi et al. concluded that 1-2 ms corresponded to the initial rearrangements, followed by significantly slower changes in the TM domain (~ 20 ms). This aligns with other studies on mGluR1 that the VFT activation occurs rapidly in few ms, while the full activation takes place in dozens of ms (e.g. Hlavackova et al. Sci Signal 2012, Marcaggi et al. PNAS 2009).

We fully agree that receptor activation involves two processes: initial inter-subunit rearrangement (protomer approximation) and subsequent intra-subunit TM conformational changes (precisely at the ICL2 and C-terminus, where the fluorescent labels in the above studies were located). The latter process, associated with G protein coupling, was beyond the scope of our original manuscript. The NEB calculations and subsequent MD sampling primarily focused on the inter-subunit rearrangement between the inactive and agonist-bound active state. The approximately 1 ms timescale for this process, as suggested by the MSM, aligns with the 1-2 ms inter-subunit rearrangement timescale in mGluR1 — not the full activation timescale of approximately 20 ms, which we have corrected following your suggestion in the last revision.

Moreover, in the last revision, we utilized AlphaFold2-multimer to generate the structure of the mGluR5-Gq complex and conducted 10 independent classical MD simulations, each lasting 1.0 μs, to investigate the full intra-subunit activation process. Despite the extensive computational efforts, these simulations are unlikely to capture the complete full activation conformational landscape upon Gq coupling. Therefore, there is no need to calculate the underlying intra-subunit activation timescale. Interestingly, the simulations do reveal significant conformational rearrangements of

the ICL2 and the C-terminus to envelop the Gq α5 helix. Please refer to the Supplementary Note 7 and 8 for the detailed information.

The comparison with the latest data on mGluR5 by the Kobilka lab (Kumar 2023 bioRxiv) also shows discrepancies. For instance, the CRD-CRD distances here appear to describe 2-3 states, whereas 4 states have been shown by Kumar et al., similar to mGluR2 (Liauw 2021 Nat Chem Biol).

Our original simulations described the first 3 states of the CRD-CRD distances. The 4th state, shown by Kumar et al., represents the fully active state in the presence of the Gq protein. Our new MD sampling of the predicted mGluR5-Gq complex also revealed this 4th distinct state (~ 35.1 Å) of the CRD-CRD distances (see Figure R3 below).

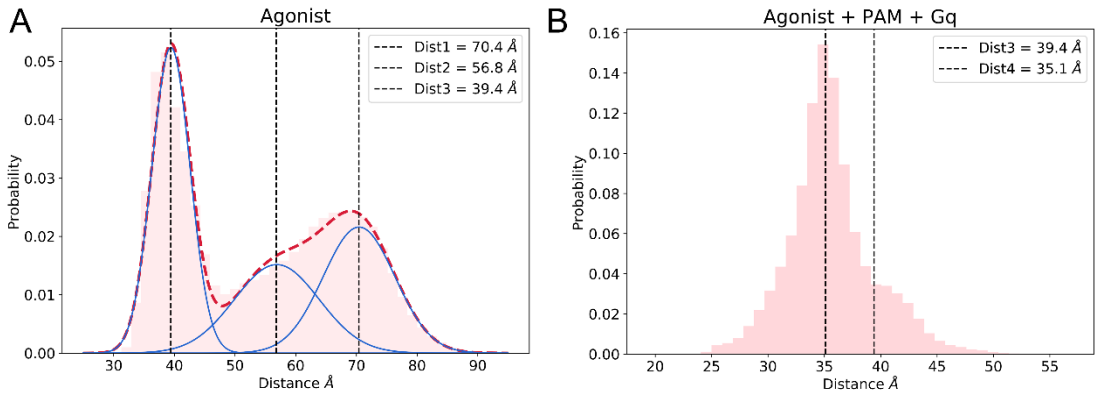

Figure R3. Conformational distributions of dD560-D560. Thin blue solid lines depict the Gaussian-fitted distributions of the three states upon only agonist loading (A) and the fully active state upon G_q coupling (B). These correspond to the four states identified in mGluR2, mGluR3 and mGluR5 through the smFRET technique, achieved by conjugating donor and acceptor fluorophores at analogous positions on the CRDs.

Fig.S3 also indicates that the 3 domains in the MD sampling have strong correlations (seemingly so from the histograms, while the correlations are not examined), rather than loosely coupled.

The correlations were quantitatively examined by the coefficient of determination (R2), which measures the strength of the relationship between the x and y values on a scale from 0 to 1, with 1 indicating perfect coupling. As a positive control, due to the inter-domain disulfide bonds linking the lower lobes of VFT and the B2' modules of CRD, a significantly tighter coupling is observed (R2 = 0.91). In contrast, the extensive simulations demonstrated that the dynamics between the VFTs and CRDs (R2 = 0.62),

as well as between the CRDs and the 7TM domains (R2 = 0.58), are loosely coupled. Please refer to the Supplementary Note 3 for the detailed information.

I hope these comments will help the authors improve the otherwise interesting study. The manuscript has merits but I do not recommend publication in its current form.

Reviewer #4 (Remarks to the Author):

Whether the transient non-crystallographic poses of glutamate observed in S1 and S2 states are physiologically relevant (on-pathway).

We thank the referee for their enthusiasm and constructive suggestions.

We would like to point out that the non-crystallographic poses of glutamate are reasonable intermediate transition states, as they eventually evolve into the classical crystallographic poses observed in the subsequent S3, S4 and S5 states (correct endpoint). These transient poses offer the first atomic-level mechanistic insights into the well-characterized, physiologically relevant, stepwise activation of the VFT domain (where glutamate binds) of mGluRs. Beyond the VFT domain, we have dedicated extensive efforts and gained novel mechanistic insights into the less characterized CRD and 7TM domains. The physiological relevance of these insights has been substantiated by our experimental signaling assays.

More importantly, mGluR5 is considerably larger than typical simple monomeric GPCR and enzyme systems, making it challenging to investigate. Our study proposes a novel and generalizable computational strategy that is readily applicable for characterizing millisecond-long events in other allosteric systems. We agree that the physiological relevance of transient glutamate binding poses is an extremely interesting avenue for future research. To this end, we have added the following sentence to the discussion:

"*the physiological effects of the identified non-classic glutamate binding poses remain an interesting question to address in future studies.*"

REVIEWERS' COMMENTS

Reviewer #5 (Remarks to the Author):

This is an interesting study that provides new information on the mechanism of mGlu5 receptor activation. The study is well designed and carried out. Computational results showing structural data for allosteric interactions between and within subunits are relevant and allow us to better understand the activation process and suggest hypotheses to be tested in future studies. Of particular interest is the identification of several intermediate states along the conformational dynamics of receptor activation and the inter-subunit transition kinetics among them. Furthermore, all-atom MD simulations of mGlu5 homodimer including glutamate and a PAM in the absence and presence of the Gq protein allowed differentiation of the G protein binding mode in the mGlu5 receptor from those found in Class A GPCRs.

Very minor typographic observation:

Please, revise the following paragraph in Page 6 and check whether “conforming that” should be replaced by “confirming that”.

The convergence of the FEL was proven with varied subsets of the MD samplings, conforming that the sampling has been sufficient to explore the mGlu5 activation (Supplementary Note 2 and Figure S2).

Reviewer #6 (Remarks to the Author):

In their manuscript, the authors performed advanced molecular dynamics simulations to capture atomistic insights into the mGlu5 receptor activation mechanism. By combining the NEB approach with MSM analysis, they were able to unravel the various stages of the mechanism and propose an activation scheme that is consistent with experimental observations. From a methodological standpoint, the analyses are sound. The authors have taken great care to justify the parameters chosen for the simulations and analyses, including the number of replicas, lag time, and choice of features, among others. I would recommend this manuscript to be published in Nature Communications. Here are some suggestions and recommendations to consider prior to publication.

Minor points:

- Fig.2.C : Why are the movements of only the transmembrane parts highlighted by the yellow arrows? It seems that the closure of the extracellular part and the rotation of the two monomers are equally important as the closure of the transmembrane part. Please adjust the figure accordingly to illustrate the full dynamics of the protein.

- Among the mutants chosen to demonstrate the role of CRD, I523C is the most informative. How was this position selected for crosslinking? Was it by chance, or was there a rational basis for this choice?

- Fig.5: Following the movements of Y6.44 and Y3.44 makes sense, as these residues have already been identified as micro-switches. However, I am puzzled by the decision to focus on M778(6.43) and not W685(6.50), which is known to play a crucial role in forming the TM6-TM6 interface upon activation. The fact that the M778(6.43) mutant has a deleterious effect on receptor response does not necessarily imply that it is a key residue in the activation mechanism. Instead, its proximity to other key residues already characterized (Y6.44, W6.50) could be sufficient to explain the effect of the M6.43 mutation.

- Fig.5.A and Fig.5.B: Where is the position of the inactive structure? Please indicate.

- Page 22: The term "saddle point" is confusing in the sentence "a partial NEB… procedure available in A20 was used to generate 32 saddle points". I believe it's not referring to saddle points, but rather 32 interpolated images (or replicas) representing the Minimum Energy Path (MEP) to be optimized.

- Page 7: mGlu5 and mGlu1 share more than 70% of sequence identity and not similarity!

Small typos:

- Page 4, end of first paragraph: “…coupling with its G protein partner?” and not “couping”.

- Fig.S12: "…front view of TM2, TM3, and TM6…" and not "TM2, TM3 and TM5". Also, please add the superscript 3.53 to R6683.53. Can the authors clarify whether monomers A and B are shown in red and blue in this figure?

- Fig.S16 : I believe there is an error involving an inversion between G1 and G3. The "fully activated" state should correspond to an open ionic lock (large distance, as shown in the pink figure - currently labeled as G1), whereas the "pre-coupled" state should correspond to a closed ionic lock (small distance, as shown in the green figure - currently labeled as G3). If my analysis is correct, all they need to do is swap the labels G1 and G3 throughout the figure.

Reviewer #5 (Remarks to the Author):

This is an interesting study that provides new information on the mechanism of mGlu5 receptor activation. The study is well designed and carried out. Computational results showing structural data for allosteric interactions between and within subunits are relevant and allow us to better understand the activation process and suggest hypotheses to be tested in future studies. Of particular interest is the identification of several intermediate states along the conformational dynamics of receptor activation and the inter-subunit transition kinetics among them. Furthermore, all-atom MD simulations of mGlu5 homodimer including glutamate and a PAM in the absence and presence of the Gq protein allowed differentiation of the G protein binding mode in the mGlu5 receptor from those found in Class A GPCRs.

RESPONSE: Thank you for your affirmation of our work, and we sincerely appreciate your meticulous review of our manuscript and your highlighting of the remaining issues. Your insightful feedback has been invaluable in enhancing the quality of our work.

Very minor typographic observation:

Please, revise the following paragraph in Page 6 and check whether “conforming that should be replaced by “confirming that”.

The convergence of the FEL was proven with varied subsets of the MD samplings, conforming that the sampling has been sufficient to explore the mGlu5 activation (Supplementary Note 2 and Figure S2).

RESPONSE: Thank you for pointing this out. The “conforming that” has been corrected to “confirming that”.

Reviewer #6 (Remarks to the Author):

In their manuscript, the authors performed advanced molecular dynamics simulations to capture atomistic insights into the mGlu5 receptor activation mechanism. By combining the NEB approach with MSM analysis, they were able to unravel the various stages of the mechanism and propose an activation scheme that is consistent with experimental observations. From a methodological standpoint, the analyses are sound. The authors have taken great care to justify the parameters chosen for the simulations and analyses, including the number of replicas, lag time, and choice of features, among others. I would recommend this manuscript to be published in Nature Communications. Here are some suggestions and recommendations to consider prior to publication.

RESPONSE: Thank you for your affirmation of our work, and we sincerely appreciate your meticulous review of our manuscript and your highlighting of the remaining issues. Your insightful feedback has been invaluable in enhancing the quality of our work.

Minor points:

- Fig. 2C: Why are the movements of only the transmembrane parts highlighted by the yellow arrows? It seems that the closure of the extracellular part and the rotation of the two monomers are equally important as the closure of the transmembrane part. Please adjust the figure accordingly to illustrate the full dynamics of the protein.

RESPONSE: We totally agree with your suggestions. The Fig. 2C has been accordingly adjusted to clearly show the full dynamics of mGlu5.

- Among the mutants chosen to demonstrate the role of CRD, I523C is the most informative. How was this position selected for crosslinking? Was it by chance, or was there a rational basis for this choice?

RESPONSE: The simulations indicated that during the dynamic CRD association, the inter-domain distance between the Cα atoms of I523 is about 5 Å. Considering that the typical distance between the two Cα atoms in a disulfide bond is about 5.6 Å (Schmidt et al., *Biochemistry*, **2006**, 45(24):7429-7433), this position was chosen strategically for crosslinking. The effectiveness of this choice was confirmed by the high constitutive activity observed in the I523C mutant.

- Fig.5: Following the movements of Y6.44 and Y3.44 makes sense, as these residues have already been identified as micro-switches. However, I am puzzled by the decision to focus on M778(6.43) and not W685(6.50), which is known to play a crucial role in forming the TM6-TM6 interface upon activation. The fact that the M778(6.43) mutant has a deleterious effect on receptor response does not necessarily imply that it is a key residue in the activation mechanism. Instead, its proximity to other key residues already characterized (Y6.44, W6.50) could be sufficient to explain the effect of the M6.43 mutation.

RESPONSE: Thank you for your insights. In this part, we aim to explore how the activation signal is transmitted from the inter-domain TM6-TM6 interface via dimerization to the intra-domain, from the perspective of micro-switches. Both simulations and experiments suggest that the formation of the TM6-TM6 interface initially and directly triggers rotamer changes in $Y779^{6.44}$, which sequentially modify its neighboring residues, $M658^{6.43}$ and the well-recognized intra-domain micro-switch, $Y659^{3.44}$. Indeed, $M658^{6.43}$ and $Y659^{3.44}$ could affect other micro-switches, such as the toggle switch $W785^{6.50}$. Given that $Y659^{3.44}$ is located closer to the G-protein binding site compared to other micro-switches, the $Y779^{6.44}$ - $M658^{6.43}$ - $Y659^{3.44}$ serves as one of the most representative pathways for transmitting the activation signal from the inter-domain interface to the intra-domain region.

- Fig.5.A and Fig.5.B: Where is the position of the inactive structure? Please indicate.

RESPONSE: We have now marked the position of the inactive structure in Fig. 5A and Fig. S11, the latter of which provides a full view of Fig. 5B.

- Page 22: The term "saddle point" is confusing in the sentence "a partial NEB... procedure available in A20 was used to generate 32 saddle points". I believe it's not referring to saddle points, but rather 32 interpolated images (or replicas) representing the Minimum Energy Path (MEP) to be optimized.

RESPONSE: Yes, the term “saddle point” has been corrected to “interpolated images”.

- Page 7: mGlu5 and mGlu1 share more than 70% of sequence identity and not similarity!

RESPONSE: Thank you for pointing this out. The “similarity” has been corrected to “identity”.

Small typos:

- Page 4, end of first paragraph: “…coupling with its G protein partner?” and not “couping”.

- Fig.S12: "...front view of TM2, TM3, and TM6..." and not "TM2, TM3 and TM5". Also, please add the superscript 3.53 to R6683.53. Can the authors clarify whether monomers A and B are shown in red and blue in this figure?

- Fig.S16: I believe there is an error involving an inversion between G1 and G3. The "fully activated" state should correspond to an open ionic lock (large distance, as shown in the pink figure - currently labeled as G1), whereas the "pre-coupled" state should correspond to a closed ionic lock (small distance, as shown in the green figure - currently labeled as G3). If my analysis is correct, all they need to do is swap the labels G1 and G3 throughout the figure.

RESPONSE: Thanks a lot, we have carefully revised the manuscript again and corrected all the typos.